

Event-Based Control Systems for Microalgae Culture in Industrial Reactors

A. Pawlowski, J.L. Guzmán, M. Berenguel, F.G. Acién and S. Dormido

Abstract In this chapter, event-based control approaches for microalgae culture in industrial reactors are evaluated. Those control systems are applied to regulate the microalgae culture growth conditions such as pH and dissolved oxygen concentration. The analyzed event-based control systems deal with sensor and actuator deadbands approaches in order to provide the desired properties of the controller. Additionally, a selective event-based scheme is evaluated for simultaneous control of pH and dissolved oxygen. In such configurations, the event-based approach provides the possibility to adapt the control system actions to the dynamic state of the controlled bioprocess. In such a way, the event-based control algorithm allows to establish a tradeoff between control performance and number of process update actions. This fact can be directly related with reduction of CO₂ injection times, what is also reflected in CO₂ losses. The application of selective event-based scheme allows the improved biomass productivity, since the controlled variables are kept within the limits for an optimal photosynthesis rate. Moreover, such a control scheme allows effective CO₂ utilization and aeration system energy minimization. The analyzed control system configurations are evaluated for both tubular and raceway photobioreactors to prove its viability for different reactor configurations as well as control system objectives. Additionally, control performance indexes have been used to show the efficiency of the event-based control approaches. The obtained results demon-

A. Pawlowski (✉) · S. Dormido
Department of Computer Science and Automatic Control, UNED, Madrid, Spain
e-mail: a.pawlowski@dia.uned.es

S. Dormido
e-mail: sdormido@dia.uned.es

J.L. Guzmán · M. Berenguel
Department of Informatics, University of Almería, ceiA3, CIESOL, Almería, Spain
e-mail: joseluis.guzman@ual.es

M. Berenguel
e-mail: beren@ual.es

F.G. Acién
Department of Chemical Engineering, University of Almería, ceiA3, CIESOL,
Almería, Spain
e-mail: facien@ual.es

strated that the analyzed control algorithms improve the microorganism growth condition and in consequence the overall production rate is increased.

1 Introduction

Microalgae have been proposed for the production of industrial commodities as biofertilizers and biofuels, in addition to CO₂ abatement and wastewater treatment processes (Acién et al. 2012; Kokossis and Yang 2010; Costache et al. 2013; Mendoza et al. 2013b). They can contain more than 50% crude protein, with a 25-fold higher yield than soybeans, and their lipids productivity is several times larger than vegetable oils. Another important factor that characterizes the microalgae process is the high cultivation rate for the surface area used in its growth (Peng et al. 2013). Moreover, microalgae have been proposed as the only alternative for the sustainable production of biodiesel and bioethanol (Chisti 2007). Nonetheless, to be competitive in the commodities, market microalgal production must approximate crop prices and become lower than 0.5 €/kg, much lower than actual production cost (Acién et al. 2012). Thus, in practice, microalgae are used today in animal feed, in addition to human nutrition, cosmetics, and in the production of high-value ingredients such as polyunsaturated fatty acids and carotenoids (Spolaore et al. 2006). The worldwide production of microalgal biomass is 9000 t dry matter per year, its price ranging from 30 to 300 €/kg, and the size of these markets is growing considerably (Brennan and Owende 2010; Charpentier 2009).

The microalgae culture can be cultivated in reactors with different architectures, providing the properties one is looking for. Closed photobioreactors are generally used when high-quality algal biomass from determined strain is required. To this end, tubular photobioreactors are frequently used. When the high production volume is prioritized over the quality, open reactors are employed. In this group, the raceway photobioreactor is the most popular, because of its low production costs and operation simplicity (Weissman and Goebel 1987). Nowadays, there are many architectures that slightly vary from original design proposed by Oswald in the 1960s (Oswald and Golueke 1960). Despite differences in the physical architecture, all of them are developed to provide optimal microalgae growth conditions. As shown in Costache et al. (2013), the most important parameters affecting microalgae culture are pH, solar irradiance, dissolved oxygen, and medium temperature. Additionally, the photosynthesis rate in microalgae growth process depends not only on solar irradiance, but also influenced by other variables resulting in a complex system.

In open configurations, such as raceway reactors, operating temperature as well as light regimen is specified by the photobioreactor architecture and cannot be changed during operation. All remaining parameters of microalgae growth process, e.g., pH and dissolved oxygen, must be managed by suitable control scheme. The dissolved oxygen and pH levels depend on the photosynthesis rate and should be maintained close to their optimal levels. Otherwise, microalgae biomass productivity will drop and in extreme cases could lead to harmful effect on microorganism conditions.

All aforementioned properties indicate the raceway reactor as a feasible solution for microalgal biomass production. Many studies were performed on the optimal raceway reactors design and architectures providing optimal conditions for the microorganism growth (Weissman et al. 1988; Richmond 2004; Chiaramonti et al. 2013; Mendoza et al. 2013b). In consequence, there exist many raceway photobioreactors designs that slightly differ from the design proposed by Oswald and Golueke (1960), providing optimal culture conditions (Chiaramonti et al. 2013; Sompech et al. 2012; Mendoza et al. 2013a, b). In spite of several layouts, the operation principle is similar and numerous factors need to be fulfilled to provide optimal biomass production rate.

Although traditionally microalgae have been cultivated in open photobioreactors due to the simplicity and low cost, when high-value algal products from defined strains are required, it is necessary to use closed photobioreactors such as tubular photobioreactors (Taras and Woinaroschy 2012). These photobioreactors allow to control the operating conditions and avoid contamination, being available to fulfill requirements for the production of biomass in food, feed, and additives (Wang et al. 2012). The main objective of the closed photobioreactor system is to obtain a high-quality biomass by adjusting the culture conditions to optimal values requested by microalgae strain used, especially pH. In tubular photobioreactors, pH control is performed by injection of pure carbon dioxide. The supply of pure carbon dioxide can constitute up to 30% of the overall microalgae production cost (Ación et al. 2012). Moreover, the carbon losses in tubular photobioreactors can be higher than 50% in extreme cases, but can be reduced below 30% through proper design and operation of the photobioreactor (Ación et al. 1999). To reduce this even further, it is necessary to design advanced control strategies that take into account the mixing and mass transfer phenomenon that occurs in the system (García et al. 2003; Sierra et al. 2008; Cai et al. 2013). Thus, the main control problem for these processes will be to regulate the system pH by simultaneously minimizing the CO₂ losses.

Next to temperature and solar irradiance, pH is one of the most important parameters that affect the photosynthesis performance. The application of CO₂ to the microalgae growth process changes the pH level due to acidity alteration of the microorganism growth medium. Moreover, the CO₂ is used also to provide the inorganic carbon to prevent carbon limitation of the photosynthesis production rate. The excess of the CO₂ significantly decreases pH, resulting in culture damage. On the contrary, CO₂ scarcity could reduce drastically the inorganic carbon availability below the required level and result in limited growth performance (Beneman et al. 1987; Berenguel et al. 2004). The use of CO₂ corresponds to the important operational cost for microalgae production process, so it could not be supplied in excess (Godos et al. 2014). Additionally, unlimited CO₂ supply lead to unnecessary emission to the atmosphere and should be optimized by control system with efficient use of resources (Beneman et al. 1987; Pawlowski et al. 2014; Bernard 2011). Using this relationship, the control technique uses the pH level to compute the time instant and the quantity of CO₂ to be supplied. For this reason, the tradeoff between minimization of carbon dioxide losses and pH regulation precision should be taken into account in the control approach. From the economic point of view, the profitabil-

ity of microalgae culture can be improved, if carbon dioxide requirement is covered using waste flue gases (Laws and Berning 1991; Putt et al. 2011; Godos et al. 2014). In this particular configuration, it is necessary to guaranty high mass transfer rates, what has been extensively studied in previous research (Putt et al. 2011; Tang et al. 2011; Godos et al. 2014). The flue gases application method can be performed using two approaches, controlled on-demand supply and continuous bubbling, respectively (Acién et al. 2012). According to the finding from Doucha et al. (2005) and Godos et al. (2014), controlled on-demand supply of waste flue gases provides improved efficiencies of the order of 33% and 66%, respectively. Otherwise, continuous bubbling technique is characterized by low efficacy of carbon dioxide usage, obtaining 4.2 and 8.1% following analysis reported in Hu et al. (1998) and Zhang et al. (2001).

All previous control techniques for pH control provided promising performance results with an adequate CO₂ losses reduction. In Fernández et al. (2010), classical PID and feedforward control strategies were developed to cope with this problem, where a simplified linear model of the pH evolution based on changes in CO₂ injection was used for control design purposes. Moreover, in Romero-García et al. (2012), an FSP (Filtered Smith Predictor) approach has been used to improve control results in the presence of significant time delay due to pH sensor location. In both cases, important improvements against on/off controllers were obtained. On the other hand, MPC (Model Predictive Control) techniques have also been used satisfactorily in pH control problems obtaining very good results (Senthil and Zainal 2012; Oblak and Skrjanc 2010; Lazar et al. 2007). An example of pH control in photobiosreactors using Generalized Predictive Controller (GPC) can be found in Berenguel et al. (2004). In that case, it was possible to improve the overall control performance respect to the classical on/off controller. This was possible, thanks to the predictive algorithm that captures the process dynamics as well as considers the on/off valve limitation explicitly in the process constraints. Besides, CO₂ losses were considerably reduced in comparison to the commonly used on/off controllers. The main advantage of MPC algorithms is their constraints handling capability, allowing to consider any physical limitations of the process as well as the used equipment. For that reason, these algorithms are very popular in chemical process control applications (Hu and Farra 2011; Christofides et al. 2013).

Another parameter that has an important influence on the photosynthesis rate is the dissolved oxygen content. High concentration indexes of this variable in the culture medium lead to a severe threat to microorganism growth. In combination with other parameters, it could provoke light-energy dissipation through photorespiration, enzyme inhibition of the photosynthetic pathways, and might cause damage to the photosynthetic apparatus, membrane structures, DNA, and other cellular components (Peng et al. 2013; Ugwu et al. 2007; Santabarbara et al. 2002; Marquez et al. 1995). In open ponds, such as raceway reactor, it is supposed that no specific control is needed for dissolved oxygen, since its excess should be transmitted to the atmosphere. Nevertheless, in practice, this assumption is not always correct, since dissolved oxygen concentration can reach as high as 500% air saturation as reported in Mendoza et al. (2013a), Peng et al. (2013). To reduce dissolved oxygen influence on microalgae growth, it is necessary to incorporate stirring mechanism or aeration.

In both techniques, it is necessary to increase the complexity of the reactor adding new equipment, what increases production and maintenance costs. Following the results from Peng et al. (2013) and Mendoza et al. (2013a), the dissolved oxygen evacuation problem is still an important challenge despite the significant technical improvements in this subject. Especially, information on large-scale reactors is insufficient, so additional research is required regarding large-scale photobioreactors with dedicated control systems (Han et al. 2012).

However, as these control algorithms are time-based control approaches, the control action is always calculated and executed on the plant even for small control errors. Thus, the control effort, and therefore the CO₂ losses, may be reduced even further if control techniques that only act when necessary (for instance, when the control error is relevant) are used. This is the case of event-based control approaches, which are becoming very popular from a practical point of view since they allow finding a tradeoff between performance and control effort in a very straightforward manner (Årzén 1999; Pawlowski et al. 2009). Due to these properties, an event-based control approach can be applied to wide range of process, since it allows to establish a tradeoff between control effort (resource utilization) and control performance.

The event-based controllers have been introduced as an alternative solution for classical control systems (Årzén 1999; Åström 2007). The main feature that differentiates event-based systems from classical approach is realtered to the ability to adapt itself to the dynamics of controlled process. Several previous works report that usage of event-based control techniques provides many advantages, especially for a wide range of bioprocesses (Beschi and Dormido 2012; Sánchez et al. 2011; Pawlowski et al. 2014). The event-based control systems become an interesting alternative for processes where the compromise (tradeoff) between usage of control resources and control system accuracy must be met. This tradeoff can be linked to economic or environmental aspects, such as energy usage minimization, fuel savings, or any other quantity that need to be optimally used (Pawlowski et al. 2012b, 2014). Some examples can be found in a recently performed work (Pawlowski et al. 2014), which study the event-based control approach applied to pH control in a tubular photobioreactor. The introduced event-based approach reduces carbon dioxide losses, and simultaneously keeping pH inside the established limits being optimal for biomass production. From the industrial production point of view, this aspect is critically important since it prevents excessive dose of waste flue gases that could provoke environmental danger. Considering aforementioned advantages of event-based approaches, in this chapter, we provide the practical evaluation of such control systems that are applied to the tubular as well as raceway industrial photobioreactors.

First analyzed strategy addresses the development and implementation of an event-based MPC algorithm to control the pH of an industrial photobioreactor. From the pH control point of view, the event-based MPC could reduce the controller attention (reducing computational costs) while limiting the resource utilization (applying new control values only if it is strictly necessary). Hence, the application of event-based control in tubular photobioreactors is motivated by reaching both, control effort reduction (minimization of CO₂ losses) and keep the pH level in a certain range. In this case, a recent event-based GPC control strategy (Pawlowski et al.

2012b) is implemented to control the pH in a tubular photobioreactor and to achieve the system requirements. The event detection is based on the level-crossing sampling technique with additional time limits (Årzén 1999). With this idea, the control actions are only calculated when the process output is outside a certain band around the set point. The control law is computed fast when events are detected and slow when there are no events. On the other hand, the controlled variable, pH, is regulated with established tolerance (determined by sensor virtual deadband), what allows to reduce the control effort (Pawlowski et al. 2015). In this configuration, the control variable (state of on/off valve) is updated only when necessary, what reduces considerably the CO₂ usage. This fact is directly reflected in CO₂ losses, which makes the event-based controller a resource-aware control system. The presented control strategy is tested on an industrial photobioreactor to verify its performance against plant-model mismatch, process disturbances, and measurement noise. Moreover, the obtained results are compared with classical on/off controllers and the classical time-based GPC.

The second analyzed approach shows the event-based control approach applied to raceway reactors for pH process control. In such application, the event-based control technique provides improved pH control accuracy, improving the growth condition of microorganisms. Additionally, the event-based GPC in combination with actuator deadband (Pawlowski et al. 2014) minimizes the injection time of flue gases. The developed event-based controller has an additional design parameter to adjust virtual actuator deadband. Additionally, the event-based predictive controller can be extended with disturbance compensation mechanism (Camacho and Bordóns 2007; Pawlowski et al. 2012a). Such a feature has significant importance in the raceway photobioreactor production process, since pH value is continuously influenced by changes in solar irradiance. Moreover, the disturbance handling mechanism implementation allows to improve the pH control accuracy as well as reduce even further the usage of flue gases. Taking into account this relationship, the value of virtual deadband is selected to meet the control performance and provide optimal conditions for microalgae growth. Simultaneously, the tested controller reduces the volume of injected flue gases as much as possible for desired accuracy. In this way, the evaluation of the control scheme is focused on the effective use of waste flue gases. The tests carried out in this study were performed on the industrial-scale raceway photobioreactor with no additional equipment (with basic setup). Anyhow, the proposed event-based controller can be coupled with other devices/techniques (e.g., such as presented in Su et al. 2008) to increase CO₂ transfer rate. Moreover, analyzed event-based GPC control system with actuator virtual deadband is compared to the commonly used control technique used for pH regulation (on/off controller, in this case) in raceway reactor. The comparison between two control techniques is performed through several performance indexes.

Finally, the event-based controller was implemented using selective control approach that can manage simultaneously pH and dissolved oxygen control (Pawlowski and Mendoza 2015; Pawlowski et al. 2016). As mentioned before, there are many aspects that have to be considered in the control system design. From the raceway reactor point of view, the most important are related to aeration

system energy minimization and effective carbon dioxide utilization (Johnsson et al. 2015). It should be highlighted that the control objectives for dissolved oxygen and pH are adversative, since CO_2 assimilation can be deteriorated by the aeration system. Due to these properties, a selective control technique is suitable for this issue, since it allows to limit undesired interactions and merge the objectives. The selective controller permits one to switch between two control approaches subject to logical criteria (Smith 2002; Liptak 2004). Moreover, the provided controller structure should manage the actuation dynamics to process state. This requirement can be satisfied using an event-based system as shown in Beschi et al. (2014), Pawlowski et al. (2012b), Beschi and Dormido (2012), and Pawlowski et al. (2014). In the presented control scheme, we consider all these properties and developed event-based controller is able to handle pH and dissolved oxygen with mentioned constraints.

2 Photobioreactors

This section describes the main information and configuration of the photobioreactors used for the experimental tests in this chapter. Furthermore, the linear models used for control designed purposes are presented.

2.1 Tubular Reactor

The pilot-scale reactor analyzed in this study is located at experimental station “Las Palmerillas” (Almería, Spain—property of CAJAMAR Foundation). The used facility is composed of ten tubular fence-type photobioreactors (detailed description can be found in Ación et al. 2001). The reactor consists of an external vertical loop with airlift pump that moves the culture medium through the vertical solar receiver made of transparent tubes and bubbling column (Fig. 1). The solar irradiance receiver loop has 0.09 m diameter and obtains a total length (horizontal) of 400 m. The reactor total volume is 2600 l and it has 0.7 m width and 19 m length. The receiver loop is designed to reduce the demand for land (occupying min. area), improve the flow, and maximize the penetration of the solar radiation. For the heat exchange and for degassing, the bubble column is used (3.5 m high and 0.4 m diameter). Entering gas and liquid flows are measured with digital meters. Additionally, dissolved oxygen, pH, and the temperature are monitored at the beginning and at the end of the receiver. The constant air flow rate of 20 l/min is applied in the column. At the entrance of solar receiver on-demand injections of pure CO_2 (5 l/min range) are performed to control the culture pH. Moreover, culture medium is recirculated at 0.9 m/s and the temperature is controlled through heat exchanger placed in the bubbling column. The strain used, *Scenedesmus almeriensis* CCAP 276/24 (freshwater), obtains high growth rate, supporting up to pH = 10 and temperature up to 45 °C, being temperature 35 °C and pH = 8 optimal for its cultivation. The microal-

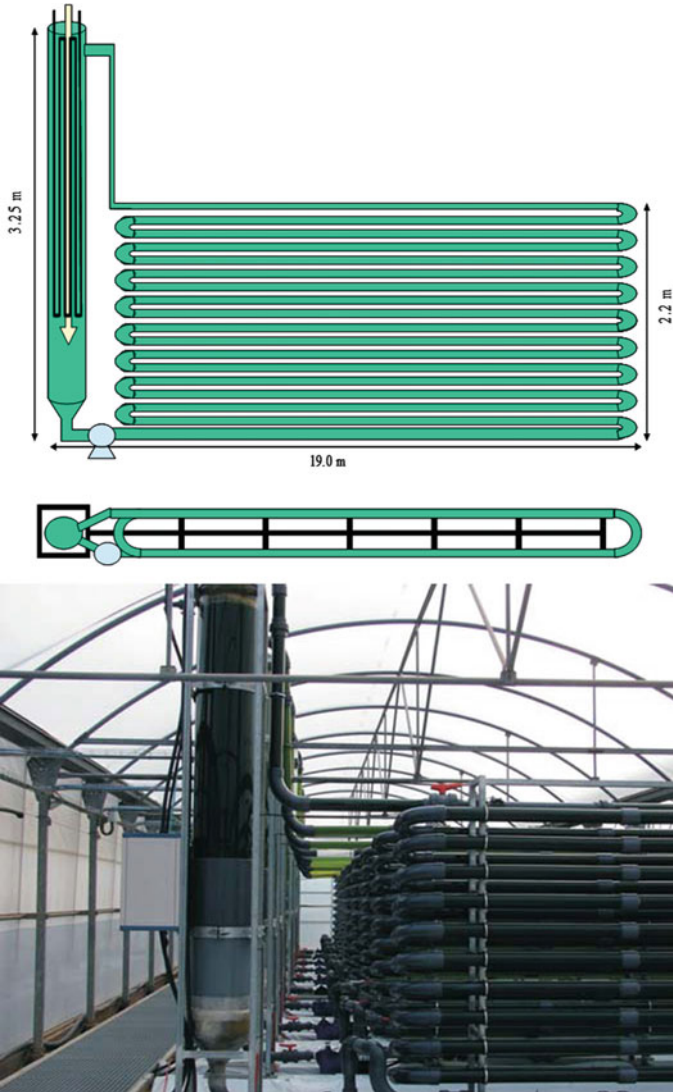


Fig. 1 Tubular photobioreactor: plane and real view (Pawlowski et al. 2014)

gae culture was cultivated in continuous mode (0.34 1/day dilution rate) and medium, Mann&Myers, and was prepared using agricultural fertilizers.

2.1.1 Linear pH Model

In order to design control system for pH variable (that rely on model predictive control approach), a simplified linear model is used. In such a process, the medium pH is influenced by CO₂ uptake and CO₂ supply that are affected by photosynthesis rate. The supplied CO₂ is used to decrease the pH level due to the formation of carbonic acid. On the contrary, the pH value gradually rises, since during photosynthesis process microalgae consume CO₂ and produce O₂ affecting medium acidity. Moreover, the photosynthesis rate depends on the solar radiation also resulting in pH changes. In this process, the pH value is the controlled variable and CO₂ supply flow is the control variable. Additionally, in such a configuration, the solar radiation is main control system disturbance. This scheme can be captured using linear model representation (Berenguel et al. 2004; Sierra et al. 2008; Fernández et al. 2010).

The parameters of such model were identified taking into account the dynamics observed in measurements and also considering distributed nature of photobioreactor architecture. The resulting model represents interaction between CO₂ injections and the pH value. Considering that microalgae culture process is nonlinear, the linear models were identified around operation point. The obtained transfer functions are as follows (Berenguel et al. 2004; Fernández et al. 2010):

$$pH = \underbrace{\frac{k_1}{1 + \tau_1 s}}_{TF_1(s)} \underbrace{\frac{\omega_n^2}{s^2 + 2\delta\omega_n s + \omega_n^2} e^{-t_r s}}_{TF_2(s)} u + \underbrace{\frac{k_r}{1 + \tau_r s}}_{TF_3(s)} I. \quad (1)$$

In this case, pH is the microalgae culture pH, u is the control variable (CO₂ supplying flow value, 0–100%), and I is the solar radiation (measurable control system disturbance). In this configuration, TF_1 is a first-order term relating input and output variable, TF_2 is used to capture recirculation effect, and t_r is a time delay present in the system due to distance between CO₂ injection point and the pH sensor. Moreover, TF_3 describes disturbance effect on the controlled variable. The final model parameters are as follows: $k_1 = -0.08$ pH %⁻¹, $\tau_1 = 28$ min, $\omega_n = 0.014$ rad s⁻¹, $\delta = 0.042$, $t_r = 7$ min, $k_r = 0.002$ pH m² W⁻¹, and $\tau_r = 182$ min. The dynamic response of the obtained model can be seen in Fig. 2, which is compared with the response of real system.

2.2 Raceways Reactor

The study for raceway reactor was performed on the pilot-scale facilities located at experimental station “Las Palmerillas” (Almería, Spain—property of CAJAMAR Foundation). Used reactor has 100 m² surface area and is composed of two 50-m-long (1 m wide) channels forming U-shape bends (see Fig. 3). The reactor operates at constant depth (0.2 m) to provide desired performance and considering power

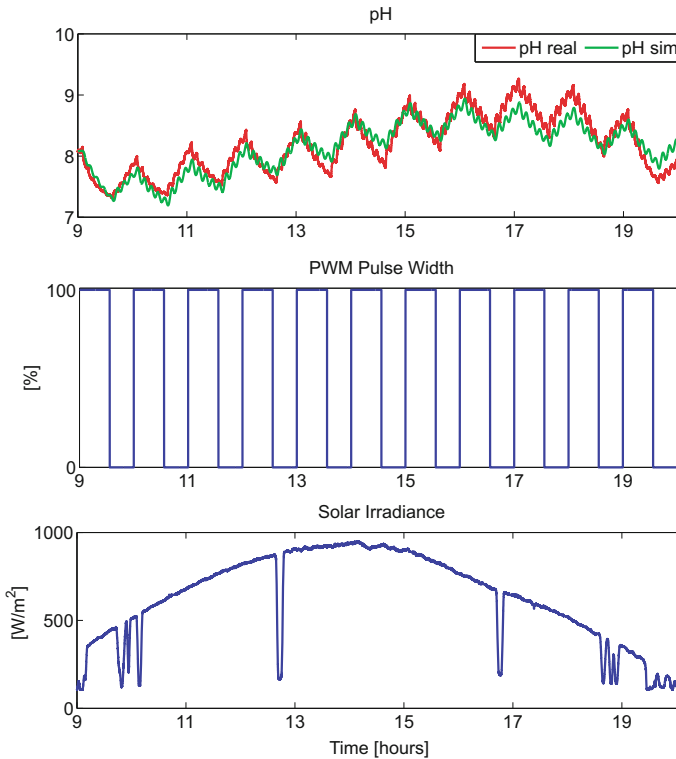
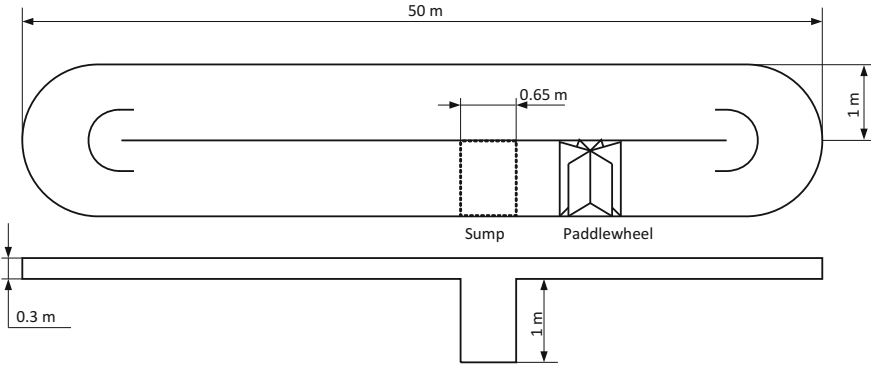


Fig. 2 Simplified model validation results for the tubular photobioreactor (Pawlowski et al. 2014)

consumption issues. Resulting reactor volume is 20 m³. Medium mixing was performed using paddlewheel (1.2 m diameter) with eight marine plywood blades at constant speed. Carbonation was done through, 1 m by 0.64 m, sump situated 1.8 m downstream the paddlewheel location. Three plate membrane diffusers were placed at the bottom of the sump and were used to inject flue gases.

The raceway photobioreactor facilities can be set up to use different carbon dioxide sources in order to provide flexible platform to evaluate different systems and techniques. Nevertheless, for the test performed in this analysis, the plant was configured to use flue gases resulting in the raceway reactor operation scheme shown in Fig. 3.

The flue gas used for pH control was taken from industrial heating boiler (diesel-fuelled with the average gas composition: 10.6% CO₂, 18.1 ppm CO, 38.3 ppm NO_x, and 0.0 ppm SO₂). In this operation scheme, exhaust gas was refrigerated to the environment temperature and stored in a 1.5-m³ pressure tank (compressed to 2 bar) with automatic regulation of pressure. The compressed flue gas was supplied to the reactor through a 150 m pipeline of 40 mm diameter. Finally, the injection system uses the solenoid on/off valve and input flow was measured with digital flow meter



(a) scheme (top and side view)



(b) real experimental facilities

Fig. 3 Raceway reactor (Pawlowski et al. 2014)

(detailed information for raceway setup can be found in Godos et al. 2014; Mendoza et al. 2013b). The injection instant as well as aperture time is provided by the control algorithm used for pH control.

Taking into account the limitation of the actuation system that is used in the pilot-scale raceway reactor, it is necessary to convert the continuous control signal into the on/off actions of solenoid control valve. To this end, PWM (Pulse Width Modulation) technique is used to translate the signal provided by the controller into train of pulses with modulated width. The value of the pulse width is determined by the control system and can vary between 0 and 100%. Moreover, the modulation frequency was set to 0.1 Hz being optimal for the main controlled variable. The conversion is performed using software procedure developed as part of a SCADA (Supervisory, Control And Data Acquisition) program.

The dissolved oxygen concentration is controlled using compressed air to evacuate its excess. The compressed air is stored in the high-pressure tank and is supplied to the raceway reactor through the sparger using on/off valve (using the same structure as for CO₂ injections). The dissolved oxygen concentration is measured using 5083T, Crison probes, MM44, and Crison transmitters.

All control techniques tested on the raceway reactor were developed in Matlab environment and implemented as a part of SCADA system. The input and output signals were governed using LabJack U12 modules from LabJack Corp.

2.2.1 Linear Process Model for pH

In the case of raceway reactor, pH process also was modeled using linear reduced-order model. As in the previous reactor type, the model structure is developed considering distribution of the actuators and sensor, the reactor architecture, and dominant dynamics in measured data. The developed model relates the carbon dioxide injections (input variable) with pH (output variable) and is given by the following structure (s represents the complex variable used in Laplace transform):

$$pH(s) = \underbrace{\frac{k_1}{1 + \tau_1 s} e^{-t_r s}}_{TF_1(s)} u(s) + \underbrace{\frac{k_r}{1 + \tau_r s}}_{TF_2(s)} v(s) \quad (2)$$

where pH is the culture medium pH, u is the control variable, and v is the solar radiation. The first term, TF_1 , relates the pH level to CO₂ injections. t_r refers to the time delay between the CO₂ injection point and the pH measure point. The TF_2 term captures the solar radiation effect on pH value, and this relationship is expressed as the first-order system. Through process identification and validation procedures, the following parameters were obtained: $k_1 = -0.005 \text{ pH}\%^{-1}$, $\tau_1 = 16.5 \text{ min}$, $t_r = 7 \text{ min}$, $k_r = 0.0007 \text{ pH m}^2 \text{ W}^{-1}$, and $\tau_r = 118 \text{ min}$. The obtained model fit can be seen in Fig. 4, where the real system data are contrasted with those obtained with developed model (Berenguel et al. 2004; Pawlowski et al. 2014).

It needs to be highlighted that during model validation stage the dissolved oxygen variable was uncontrolled (see the third plot in Fig. 4). From this plot, it can be observed that its measured value reach 400 [%Sat], being significantly over the value that guarantees efficient photosynthesis process. This simple example shows the necessity to develop a control system to deal with this issue. Notice that the pH and dissolved oxygen values are decoupled from the control system point of view, since there is no mutual interaction.

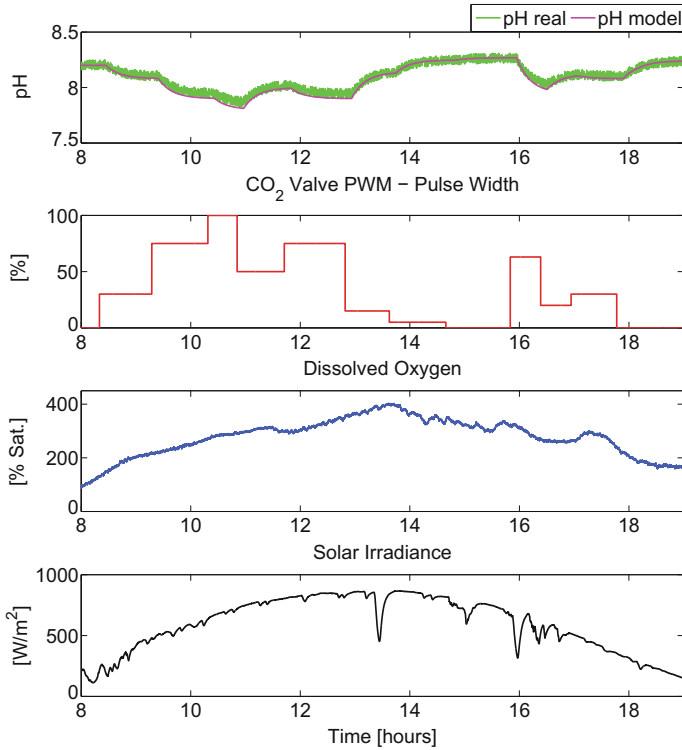


Fig. 4 Simplified model validation results for the raceway photobioreactor (Pawlowski and Mendoza 2015)

3 Control System Objectives

The analysis presented in this chapter focuses on the dissolved oxygen and pH parameters and it is supposed that remaining variables are satisfied through proper photobioreactor design. In this section, detailed information regarding dissolved oxygen and pH effect on the photosynthesis performance is provided. In the previous work (Costache et al. 2013), it was shown that the pH in the 7.0–9.0 range is optimal for the photosynthesis performance. From Fig. 5, it can be observed that in this pH range only insignificant variations in photosynthesis rate were measured. This relationship can be modeled using an Arrhenius expression of the following form:

$$RO2(pH) = B_1 e^{\left(\frac{-C_1}{pH}\right)} B_2 e^{\left(\frac{-C_2}{pH}\right)},$$

where the photosynthesis rate ($RO2$) and $B_1 = 2.50$, $B_2 = 533$, $C_1 = 6.45$, and $C_2 = 69.2$ were obtained by fitting experimental data (Costache et al. 2013).

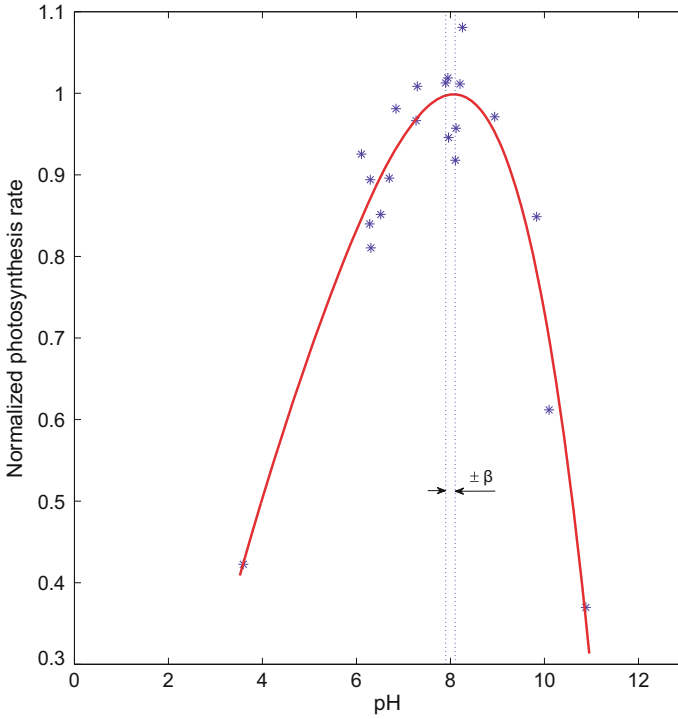


Fig. 5 The photosynthesis rate versus pH of *S. almeriensis* culture at $200 \mu\text{E}/\text{m}^2\text{s}$ 25°C , and 100 %Sat of dissolved oxygen (Pawlowski and Mendoza 2015)

Taking into account these features in the control system design, it is possible to regulate the pH around 8 using carbon dioxide injections as a manipulated variable. In Pawlowski et al. (2014), it was demonstrated that slight deviation in reference tracking could provide some benefit for control system goals. The small tolerance (marked as β in Fig. 5) in pH control accuracy does not affect the photosynthesis performance. Due to this property and exploiting event-based control system, it was possible to determine a tradeoff between the injected volume of CO_2 and control performance. Additionally, it should be highlighted that the control of pH level in a raceway reactor is performed using waste flue gases as the carbon dioxide source. For this reason, its usage should be optimized restricting its overdosage.

The relationship between the photosynthesis rate and dissolved oxygen concentration is presented in Fig. 6. As demonstrated in Costache et al. 2013, at dissolved oxygen concentrations lower or equal to saturation (9.0 [mg/l], 100 [%Sat]), the photosynthesis rate is optimal. Nevertheless, dissolved oxygen concentration at higher level reduces exponentially photosynthesis rate reaching zero above (32 [mg/l], 355 [%Sat]), see Fig. 6 for details. The dependence between dissolved oxygen (DO) and the photosynthesis rate can be expressed as follows:

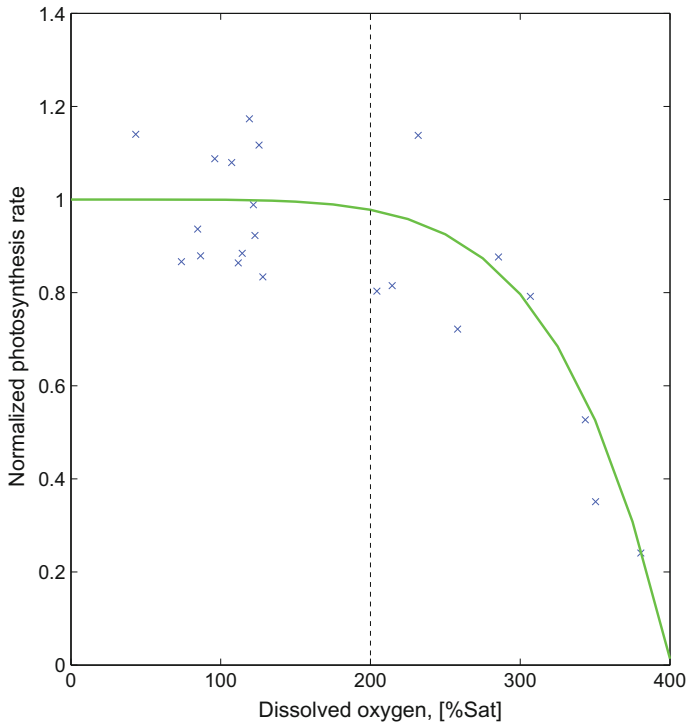


Fig. 6 The photosynthesis rate versus dissolved oxygen concentration of *S. almeriensis* culture at $200 \mu\text{E}/\text{m}^2\text{s}$, 25°C , and $\text{pH} = 8$ (Pawlowski and Mendoza 2015)

$$RO_2(DO_2) = 1 - \left(\frac{DO_2}{KO_2} \right)^z,$$

where $KO_2 = 32.8$ [mg/l] is the oxygen inhibition constant, and $z = 5.49$ (as reported in Costache et al. 2013). Moreover, the photosynthesis performance decreases only 20%, when dissolved oxygen concentration is up to values of 23 [mg/l] (250 [%Sat]), and above this level the reduction is significantly greater. For this reason, high dissolved oxygen concentration (above 250 [%Sat]) must be evaded irrespective of reactor configuration (Costache et al. 2013; Posten 2009; Camacho et al. 1999). To avoid this situation, the aeration techniques are commonly used. The most important disadvantage of such solution is related to the energy used to supply and compress the air. This issue is of high importance for raceway photobioreactors maintenance costs, since they must be kept low. Considering these facts, application of on-demand injection scheme through a proper control approach is the feasible solution from an economic point of view.

4 Event-Based Control Systems for Microalgae Culture

The event-based control schemes evaluated in this chapter are based on the GPC algorithm with sensor and actuator deadbands, originally published in Pawlowski et al. (2012b, 2014), respectively. Both approaches have been modified, to cope with microalgae culture in industrial photobioreactor. Additionally, the selective event-based approach introduced in Pawlowski and Mendoza (2015) was adapted to cope with simultaneous control of pH and dissolved oxygen within event-based scheme.

The main difference between the event-based and the time-based controller is the ability to adapt the controllers invocation, based on the controlled variable dynamics. In a control system with sensor deadband, the event-based controller will update the system in a fast way, when the controlled variable is an outside established band. Otherwise, when the controlled variable is inside the band, the event-based controller will switch to the slowest sampling in order to reduce the control effort. Considering this working principle, the event-based control structure can manage the control effort adapting it to the performance requirements of the controlled process. In a case of actuator deadband, the main idea consists of a control structure where the control signal is updated in an asynchronous manner. The main goal is to reduce the number of control signal updates, saving system resources, while retaining acceptable control performance.

4.1 Classic Generalized Predictive Controller

The Generalized Predictive Control (GPC) consists of applying a control sequence that minimizes a multistage cost function of the following form:

$$J = \sum_{j=N_1}^{N_2} [\hat{y}(t+j|t) - w(t+j)]^2 + \sum_{j=1}^{N_u} \lambda(j) [\Delta u(t+j-1)]^2, \quad (3)$$

where $\hat{y}(t+j|t)$ is an optimum j step ahead prediction of the system output on data up to time t , $\Delta u(t+j)$ is the future control signal increments, N_1 and N_2 are the minimum and maximum prediction horizons, N_u is the control horizon, $\lambda(j)$ is the control effort weighting sequence, and $w(t+j)$ is the future reference trajectory (Camacho and Bordóns 2007).

The minimum of J , assuming there are no constraints on the control signals, can be found by making the gradient of J equal to zero. Nevertheless, most physical processes are subjected to constraints and the optimal solution can be obtained by minimizing the quadratic function:

$$J(\mathbf{u}) = (\mathbf{Gu} + \mathbf{Pv} + \mathbf{f} - \mathbf{w})^T (\mathbf{Gu} + \mathbf{Pv} + \mathbf{f} - \mathbf{w}) + \lambda \mathbf{u}^T \mathbf{u}, \quad (4)$$

where \mathbf{G} and \mathbf{P} are the matrices containing coefficients of the input–output and disturbance–output step responses, respectively, \mathbf{f} is the free response of the system, \mathbf{w} is the future reference trajectory, \mathbf{u} is the control signal, and \mathbf{v} is the measurable disturbance (Pawlowski et al. 2012a, 2016). Equation (4) can be written in quadratic function form:

$$J(\mathbf{u}) = \frac{1}{2} \mathbf{u}^T \mathbf{H} \mathbf{u} + \mathbf{b}^T \mathbf{u} + \mathbf{f}_0, \quad (5)$$

where $\mathbf{H} = 2(\mathbf{G}^T \mathbf{G} + \lambda \mathbf{I})$, $\mathbf{b}^T = 2((\mathbf{P}\mathbf{v} + \mathbf{f} - \mathbf{w})^T \mathbf{G})$, and $\mathbf{f}_0 = (\mathbf{P}\mathbf{v} + \mathbf{f} - \mathbf{w})^T (\mathbf{P}\mathbf{v} + \mathbf{f} - \mathbf{w})$. The obtained quadratic function is minimized, subject to system constraints, and a classical Quadratic Programming (QP) problem must be solved. The constraints acting on a process can originate from amplitude limits in the control signal, slew rate limits of the actuator, and limits on the output signals, and can be expressed in the short form as $\mathbf{R}\Delta\mathbf{u} \leq \mathbf{r}$ (Camacho and Bordóns 2007).

4.2 Event-Based GPC with Sensor Deadband

This section briefly summarizes the event-based GPC algorithm used in this analysis and that was developed in Pawlowski et al. (2012b). In a general way, an event-based controller consists of two parts: an event detector and a controller (Åström 2007). The event detector deals with informing the controller when a new control signal must be calculated due to the occurrence of a new event. In this scheme, the controller is composed of a set of GPC controllers, in such a way that one of them will be selected according to the time instant when a new event is detected, such as described below. The complete control structure is shown in Fig. 7, including the process, the actuator, the controller, and the event generator. This scheme operates using the following ideas:

- The process output is sampled using a constant sampling time T_{base} at the event generator block, while the control action is computed and applied to the process using a variable sampling time T_f , which is determined by an event occurrence.
- T_f is the multiple of T_{base} ($T_f = fT_{base}, f \in [1, n_{max}]$) and verifies $T_f \leq T_{max}$, being $T_{max} = n_{max}T_{base}$ the maximum sampling time value. This maximum sampling time will be chosen to maintain a minimum performance and stability margins.
- T_{base} and T_{max} are defined considering process data and closed-loop specifications, following classical methods for sampling time choice.
- After applying a control action at time t , the process output is monitored by the event generator block at each base sampling time, T_{base} . This information is used by the event detector block, which verifies if the process output satisfies some specific conditions. If these conditions are satisfied, an event is generated with a sampling period T_f and a new control action is computed. Otherwise, the control action is only computed by a timing event, at $t = t + T_{max}$.
- Notice that according to the previous description, the control actions will be computed based on a variable sampling time, T_f . For that reason, a set of GPC con-

trollers is used, where each GPC controller is designed for a specific sampling time $T_f = fT_{base}, f \in [1, n_{max}]$. On the other hand, resampling of the signals is necessary to avoid undesirable jumps in the control action at each change among controllers.

4.2.1 Event-Based Signal Sampling

From the scheme in Fig. 7, it can be seen that the event-based sampling is governed by the event generator block. This block includes two different kinds of conditions in order to generate new events. When one of those conditions becomes true, a new event is generated, and then the current signal values of the process variables are transmitted to the controller block being used to compute a new control action (CO₂ injections in this case). The first condition focuses on checking the process variables. These conditions are based on the level-crossing sampling technique (Miskowicz 2006; Ferre et al. 2010), that is, a new event is considered when the absolute value between two signals is bigger than a specific limit β . For instance, in the case of the set point tracking, the condition would be the following:

$$|w(t) - y(t)| > \beta \quad (6)$$

trying to detect that the process output, $y(t) = pH(t)$, is tracking the reference, $w(t) = w_{pH}(t)$, within a specific tolerance β . The second condition is a time-based condition, used for stability and performance reasons. This condition defines that the maximum period of time between two control signals computation, and thus between two consecutive events, is given by T_{max} :

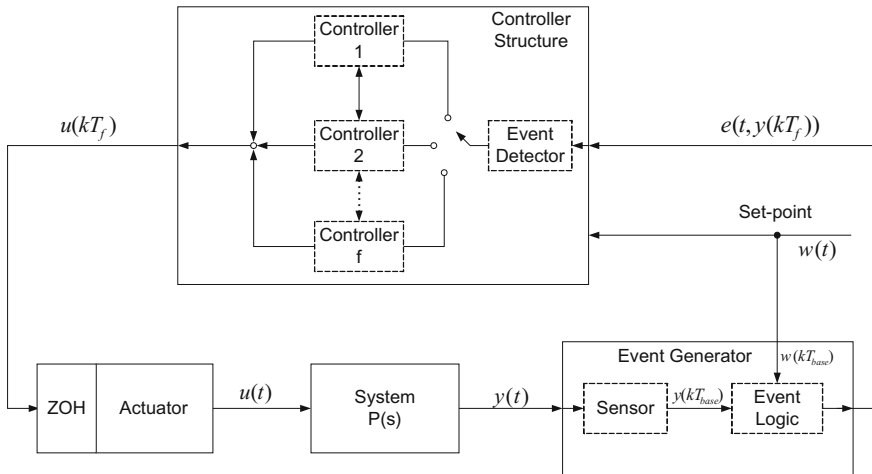


Fig. 7 Event-based GPC control scheme (Pawlowski et al. 2012b)

$$t - t_{e_i} \geq T_{max}, \quad (7)$$

where t_{e_i} is the time when the last event e_i was generated.

These conditions are checked with the smallest sampling rate T_{base} , where the detection of an event will be given within a variable sampling time $T_f = fT_{base}$, $f \in [1, n_{max}]$. Notice that this variable sampling period determines the current closed-loop sampling time to be used in the computation of the new control action.

4.2.2 Signal Sampling and Resampling Technique

Such as described above, the computation of a new control action is done with a variable sampling period T_f . So, in order to implement the GPC control algorithm, the past values of the process variables and those of the control signals must be available sampled with T_f . Therefore, a resampling of the corresponding signals is required (Pawlowski et al. 2012b, 2014b).

- Resampling of process output: As discussed previously, the controller block only receives the new state of the process output when a new event is generated. This information is stored in the controller block and is resampled to generate a vector y^b including the past values of the process output with T_{base} samples. The resampling of the process output is performed by using a linear approximation between two consecutive events and afterward, this linear approximation is sampled with the T_{base} sampling period, resulting in $y^b(k)$ with $k = 0, T_{base}, 2T_{base}, 3T_{base}, \dots$. Once the process output signal is resampled, the required past information must be obtained according to the new sampling time T_f , resulting in a new signal, y^f , with the past information of the process output every T_f samples.

Hence, the vector y^f is obtained as a result, which contains the past process information with the new sampling period T_f to be used in the calculation of the current control action.

- Reconstruction of past control signals: The procedure is similar to that described for the resampling of the process output. There is a control signal, u^b , which is always used to store the control signal values every T_{base} samples. Nevertheless, the procedure for the control signal is done in the opposite way than for the process output. First, the required past information is calculated and afterward, the signal u^b is updated. Let us consider that a new event is generated, what results in a new sampling period $T_f = fT_{base}$. Now, the past information for the new sampling period, T_f , is first calculated from the past values in u^b and stored in a variable called u_p^f . Afterward, this information, together with the past process output data given by y^f , will be used to calculate the new control action, $u^f(T_f) = u^b(k)$. Once the new control action has been computed, $u^f(T_f) = u^b(k)$, the u^b signal is updated by keeping constant the values between the two consecutive events.

4.3 Event-Based GPC with Actuator Deadband

The basic motivation to develop this approach is related to control scheme where the controlled process is updated on an asynchronous basis. The objective is to decrease the amount of control signal changes (reducing resource utilization) simultaneously providing required control accuracy. The actuator virtual deadband is implemented as a constraint on control signal changes: $|\Delta u(t)| = |u(t-1) - u(t)| \geq \beta_u$, where β_u is the proposed virtual deadband. In such a scheme, the virtual deadband value is used as an additional degree of freedom in controller tuning procedure. Its value will determine the amount of events related to actuator node, resulting in reduced number of control signal transmissions. In analyzed scheme, the proposed actuator deadband is considered in process model and consequently used in the control signal computation (MPC optimization procedure), which improves control accuracy of event-based approach.

The methodology used in this scheme consists of including the actuator virtual deadband into the GPC design framework (Pawlowski et al. 2014). The deadband nonlinearity can be handled together with other constraints on controlled process. The deadband can be expressed mathematically with a hybrid design framework developed by Bemporad and Morari (1999), which allows to translate discrete rules into a set of linear logical constraints. The resulting formulation consists in a system containing continuous and discrete components, which is known as a Mixed Logical Dynamic (MLD) system (Bemporad and Morari 1999).

Introducing two logical variables, φ_1 and φ_2 , to determine a condition on control signal increments, $\Delta u(t)$, these logical variables are used to describe the different stages of the control signal with respect to the deadband, as follows:

$$x(t) = \begin{cases} \Delta u(t) : \Delta u(t) \geq \beta_u & \varphi_2 = 1 \\ 0 : \Delta u(t) \leq \beta_u & \varphi_2 = 0 \\ 0 : \Delta u(t) \geq -\beta_u & \varphi_1 = 0 \\ \Delta u(t) : \Delta u(t) \leq -\beta_u & \varphi_1 = 1 \end{cases} \quad (8)$$

To make this solution more general, minimal m and maximal M values for control signal increments are included into the control system design procedure, resulting in $M = \max\{\Delta u(t)\}$ and $m = \min\{\Delta u(t)\}$. In this way, it is possible to determine the solution region based on binary variables. Thus, the proposed logic determined by Eq. (8) can be translated into a set of *mixed-integer linear inequalities* involving both continuous, $\Delta u \in \mathbb{R}$, and logical variables $\varphi_i \in \{0, 1\}$. Finally, a set of mixed-integer linear inequalities constraints for the actuator deadband is established as follows:

$$\begin{aligned}
\Delta u - (M - \beta_u)\varphi_2 &\leq \beta_u \\
\Delta u + (M + \beta_u)\varphi_1 &\leq M \\
\Delta u - M\varphi_2 &\leq 0 \\
-\Delta u + (m + \beta_u)\varphi_1 &\leq \beta_u \\
-\Delta u - (m - \beta_u)\varphi_2 &\leq -m \\
-\Delta u + m\varphi_1 &\leq 0 \\
\varphi_1 + \varphi_2 &\leq 1.
\end{aligned}$$

The reformulated hybrid input constraints presented above are integrated in the GPC optimization problem, where the resulting formulation belongs to an MIQP optimization problem. In the case where the control horizon is $N_u > 1$, the corresponding matrix becomes

$$\underbrace{\begin{bmatrix} \mathbf{1D} & \mathbf{0D} & -(M - \beta_u)\mathbf{D} \\ \mathbf{1D} & (M + \beta_u)\mathbf{D} & \mathbf{0D} \\ \mathbf{1D} & \mathbf{0D} & -M\mathbf{D} \\ -\mathbf{1D} & (m + \beta_u)\mathbf{D} & \mathbf{0D} \\ -\mathbf{1D} & \mathbf{0D} & -(m - \beta_u)\mathbf{D} \\ -\mathbf{1D} & m\mathbf{D} & \mathbf{0D} \\ \mathbf{0D} & \mathbf{1D} & \mathbf{1D} \end{bmatrix}}_C \underbrace{\begin{bmatrix} \Delta u \mathbf{d} \\ \varphi_1 \mathbf{d} \\ \varphi_2 \mathbf{d} \end{bmatrix}}_x \leq \underbrace{\begin{bmatrix} \beta_u \mathbf{d} \\ M \mathbf{d} \\ \mathbf{0d} \\ \beta_u \mathbf{d} \\ -m \mathbf{d} \\ \mathbf{0d} \\ \mathbf{1d} \end{bmatrix}}_\rho,$$

where \mathbf{D} is a matrix ($N_u \times N_u$) of ones and \mathbf{d} is a vector of ones with size ($N_u \times 1$). The previous matrices that contain linear inequality constraints can be expressed in a general form as

$$Cx \leq \rho \quad (9)$$

with $x = [x_c, x_d]^T$, where x_c represents the continuous variables Δu and x_d are those of the logical variables φ_i . Introducing the matrix $\mathbf{Q}_{(3N_u \times 3N_u)}$ and $\mathbf{I}_{(3N_u \times 1)}$ defined as

$$\mathbf{Q} = \begin{bmatrix} \mathbf{H} & \mathbf{0} & \mathbf{0} \\ \mathbf{0} & \mathbf{0} & \mathbf{0} \\ \mathbf{0} & \mathbf{0} & \mathbf{0} \end{bmatrix}; \mathbf{I} = \begin{bmatrix} \mathbf{b} \\ \hat{\mathbf{0}} \\ \hat{\mathbf{0}} \end{bmatrix}, \quad (10)$$

where $\mathbf{0} = N_u \times N_u$, $\hat{\mathbf{0}} = N_u \times 1$ both of zeros, \mathbf{H} and \mathbf{b} are matrices used in classical QP optimization, the GPC optimization problem is expressed as

$$\min_x x^T \mathbf{Q} x + \mathbf{I}^T x \quad (11)$$

subject to (9), which is a *Mixed-Integer Quadratic Programming* (MIQP) optimization problem (Bemporad and Morari 1999). The optimization problem involves a quadratic objective function and a set of mixed linear inequalities. Moreover, the classical set of constraints $\mathbf{R}\Delta u \leq \mathbf{r}$ can also be included into the optimization procedure, introducing an auxiliary matrix \hat{R} of the form $[R \ \bar{\mathbf{0}} \ \bar{\mathbf{0}}]$, where $\bar{\mathbf{0}}$ is a matrix of

zeros with the same dimensions that R . Finally, all constraints that must be considered into the optimization procedure are grouped in

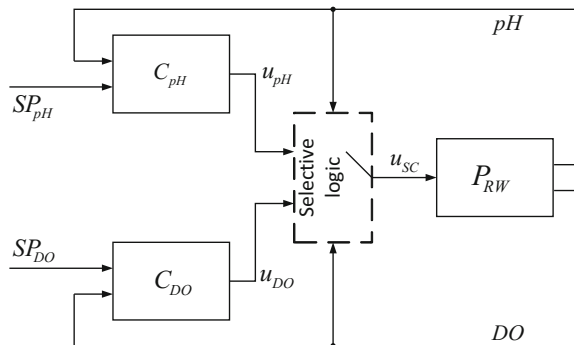
$$\begin{bmatrix} C \\ \hat{R} \end{bmatrix} x \leq \begin{bmatrix} \rho \\ r \end{bmatrix}.$$

In such a way, the event-based GPC with actuator deadband obtains optimal control signal values considering established deadband and classical constraints.

4.4 Event-Based Selective Control

Considering all aforementioned system aspects, it is necessary to meet all goals through proper control strategy, simultaneously increasing the biomass production performance handling process limitations. Taking into account process features and raceway photobioreactor configuration classical MIMO (Multiple-Input-Multiple-Output), control approach cannot be applied. However, MIMO control approach can be feasible for new reactor design that provides necessary features and solutions. Due to these properties, a selective control is considered for dissolved oxygen and pH control allowing simultaneous control of both variables. Additionally, this control technique is commonly used for controller synchronization in the systems where many control goals exist and all controllers use only one control variable (Liptak 2004). Through a selective control application, it is possible to commute between several controllers in order to optimize controlled process (Smith 2002). Exploiting these features, selective control algorithm can be used to commute between pH and dissolved oxygen controllers simultaneously meeting the control objectives. The developed selective control approach is shown in Fig. 8. From the provided scheme, it can be observed that dissolved oxygen and pH are handled with corresponding controllers, C_{DO} and C_{pH} , respectively. These controllers compute corresponding control action, given as u_{pH} and u_{DO} signals. However, the control signal application

Fig. 8 Selective control scheme for raceway reactor (Pawlowski and Mendoza 2015)



is managed by selective logic (selective mechanism), which determines the signal to be sent to the process (P_{RW}). In the presented approach, the event-based scheme is used to implement selective logic allowing dynamical adaptation to plant state. In the selective mechanism, a deadband sampling technique is used, being very common sampling approach in event-based systems. Finally, the control signal is selected in the following way:

$$u_{SC} = \begin{cases} u_{pH} : |SCSP_{pH} - pH| > \beta \\ u_{DO} : |SCSP_{pH} - pH| < \beta \ \& \ DO > SCSP_{DO} \end{cases} \quad (12)$$

where $SCSP_{DO}$ and $SCSP_{pH}$ are the set points for dissolved oxygen and pH, respectively, β determines the deadband value (control tolerance) for pH control, and DO and pH are the dissolved oxygen and pH and DO values, respectively. Due to these selection criteria, the control signal for pH variable is prioritized always when pH measurement is outside the established band. On the contrary, when pH is inside the band, the selective logic will switch to dissolved oxygen controller.

The selective control structure is developed using previously described scheme. In this configuration, the pH controller uses the event-based approach, which is built on the generalized predictive control using actuator virtual deadband (refer to Sect. 4.3) (Pawlowski et al. 2014). Moreover, the dissolved oxygen control system is based on on/off regulator. This scheme was used due to its simplicity that matches the equipment available for dissolved oxygen control—on/off solenoid valve. In the presented scheme, both pH and dissolved oxygen control systems use the reactor hardware setup with only small modifications in its original structure. The economic cost of performed modifications is negligible regarding the overall economics of the raceway reactor design and operation, since no structural modification was required. For these reasons, both control tasks share the photobioreactor systems in order to perform dissolved oxygen and pH control actions. Considering all these properties, it is possible to separate two reasons why simultaneous control of dissolved oxygen and pH is limited:

- The first reason is related to specific control system goals and limitations in microorganism cultivation system. The photobioreactor pH level is regulated applying CO_2 injections, which affects the acidity of cultivation medium. The carbon dioxide source can vary and depends on the reactor type and final product requirements. Nevertheless, independent on CO_2 source, the volume of injected gas should be optimized to prevent unnecessary emissions and thus environmental contamination. Moreover, dissolved oxygen control focuses on the evacuation of excess oxygen production that appears as a consequence of photosynthesis process. In dissolved oxygen control task, compressed air is injected to the raceway photobioreactor, which results in the reduction of oxygen saturation in cultivation medium. Due to this working principle, the control objectives for pH and dissolved oxygen are antithetical. In the described scenario, the injected air, used to reduce the dissolved oxygen concentration, can also evacuate carbon dioxide not absorbed

by the microorganism. Beside this relationship, both variables present no mutual interference and are decoupled from a control point of view.

- The second refers to the raceway photobioreactor architecture and it is related to application method of the compressed air and the flue gases. As highlighted previously, both subsystems share the same supply structure for economic reasons. The supply structure can commute when necessary and only one quantity can be supplied and only one variable can be controlled. Due to these properties, microalgae production process can be modeled as underactuated system with single input and multiple outputs (Freudenberg and Middleton 1999; Soria-López et al. 2013).

4.5 On/Off Controller

In the analysis presented in this chapter, the on/off controller is used as a reference control system, since it is the most commonly used controller in photobioreactor production process. The on/off controller is the most simple feedback regulator and it is suitable for the manipulated variable characterized by two states: open (on) and closed (off). The on/off regulator commutes the state of manipulated variable as a function of the set point and process output measurement. The most important drawbacks of this control technique are related to a poor disturbance rejection performance and oscillations around reference in controlled variables.

5 Control System Results

In this section, the results for practical evaluation of event-based control schemes for industrial photobioreactors are presented. This study considers three different configurations that are analyzed below.

5.1 Event-Based Controller pH in Tubular Photobioreactor

This section shows real experiments using the event-based control strategy applied to pH control in tubular photobioreactor described in Sect. 2.1. A preliminary simulation study on this event-based approach can be found in Pawlowski et al. (2014). Notice that in all considered control systems the continuous signal obtained from the controller must be translated into a discontinuous signal used to drive the valve. For this purpose, a PWM (Pulse Width Modulation) technique is used, with a frequency of 0.1 Hz. Notice that microalgae growth requires that the operation variables must be maintained at optimum values, where for the microalgae used in this evaluation, *Scenedesmus almeriensis*, an optimal value of $w_{pH} = 8$ is required.

As mentioned previously, the experiments are performed using the event-based GPC and the classical time-based GPC to control pH in an industrial tubular photobioreactor. The experiments have been performed between June 6 and 12, 2013, at the plant described in Sect. 2.1. During this period, the photobioreactor plant worked in the continuous mode. In this mode, 34% of the total volume of culture is harvested daily. The harvesting operation is done usually around midday and this influences on the pH value. From the control system point of view, this issue is considered as an unmeasurable disturbance, since the harvesting operation is performed by the plant operator to cover product demand. All control schemes are implemented on an industrial PC located at the plant facilities. The controller with Labview-based software executes the event-based GPC controller or classical GPC, which are coded in the Matlab environment. All control system sensors and actuators are connected to the Compact-FieldPoint unit from National Instruments. In such configuration, the controller node communicates with Compact-FieldPoint through a dedicated ethernet network to perform sensing and control tasks.

The first tested control scheme was the classical time-based GPC and was developed using model presented in Sect. 2.1.1. The control system configuration and algorithm tuning parameters are as follows: sampling time of 1 min was used with the following parameters: $N_u = 5$, $N_2 = 20$, and $\lambda = 0.005$. The value of the solar irradiance in the prediction horizon is considered constant and equals to the last measured value. This configuration was implemented and tested to assure the proper control system configuration and check the control performance in the presence of measurement noise and external disturbances that affect controlled variable. Prior to the controller implementation, several tests were made to confirm the proper model validation around the operation point. This procedure confirmed the relatively good accuracy of model (see Sect. 2.1.1), to guarantee the desired control performance.

The time-based GPC was tested during two different days and representative results of one of those days are shown in Fig. 9 (notice that classical GPC was already studied by the authors in the previous works and for that reason it was only used here for comparisons Berenguel et al. 2004). It can be observed how GPC controller regulates the pH of the photobioreactor compensating the influence of the solar irradiance (main control system disturbance). On the other hand, it can be observed how the controller reacts to the unmeasurable process disturbances (harvesting operation), between 12 and 15 h. It can be also seen that despite of the disturbance, the controller maintains the pH close to the set point, due to aggressive compensation of the control signal. During this day, the classical GPC obtains a good control accuracy, comparable with the results obtained through simulations, what was confirmed by $IAE = 1357$ index. The accumulated IT reaches 342 min that corresponds to 1262 g of pure CO_2 . To achieve this performance, an amount of 350 g of CO_2 was lost. The microalgae growth performance indexes for RO_2 and P_b were 0.7509 [$kg_{[O_2]}/m^3$ day] and 0.5572 [$kg_{[b]}/m^3$ day], respectively.

For this particular day, the classical GPC obtains a good accuracy in pH regulation. However, this good control performance is obtained through a high CO_2 consumption, what also increases the CO_2 losses. This fact confirms the results obtained through simulations. As mentioned previously, the CO_2 loss is an important issue in

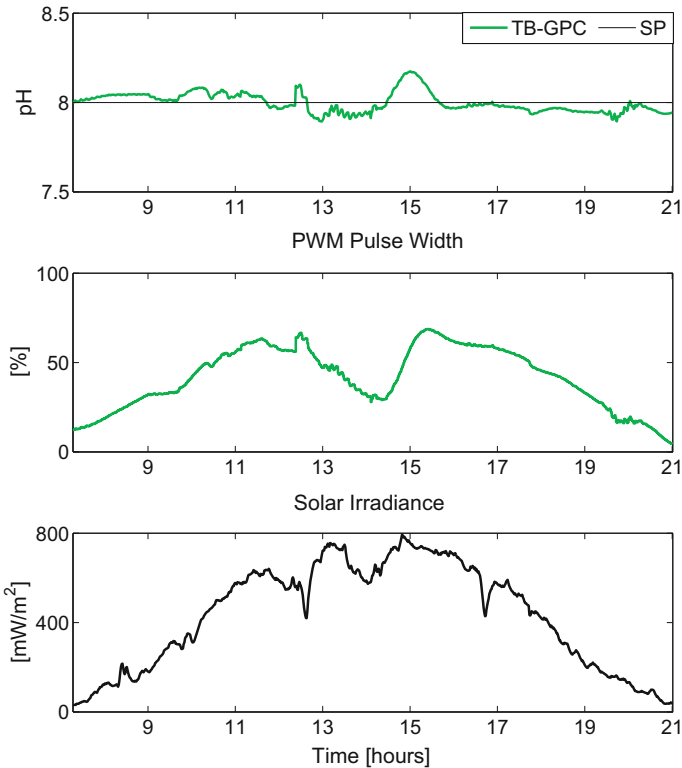


Fig. 9 Experiments control results for classical time-based GPC (Pawlowski et al. 2014)

photobioreactor pH control problem and any solution that faces this problem is welcomed. In such perspective, the event-based GPC arises as an interesting option to reduce the control effort at the expense of a reasonable control performance accuracy degradation.

The event-based GPC algorithm was implemented with the same configuration parameters as in the simulation study. Again, the control objective is to maintain the pH value close to the set point with the desired tolerance. Such a tolerance is determined by the sensor deadband value, selected to $\beta = 0.075$ for whole test period according to the relationship between the pH and the photosynthesis rate described in Sect. 3. The application of the event-based controller makes possible to establish the tradeoff between control performance accuracy and CO_2 losses.

The event-based configuration has been tested during 5 days and the overall control performance is shown in Fig. 10. The event-based GPC control structure with sensor deadband was implemented with $T_{base} = 1$ min, $T_{max} = 5$ min, $n_{max} = 5$, and thus $T_f \in [1, 2, 3, 4, 5]$. The control horizon was selected to $N_u^{n_{max}} = 5$ samples for all GPC controllers. The prediction horizon was set to $N_2^c = 20$ min in continuous time and was used to calculate the equivalent prediction horizon for each controller with

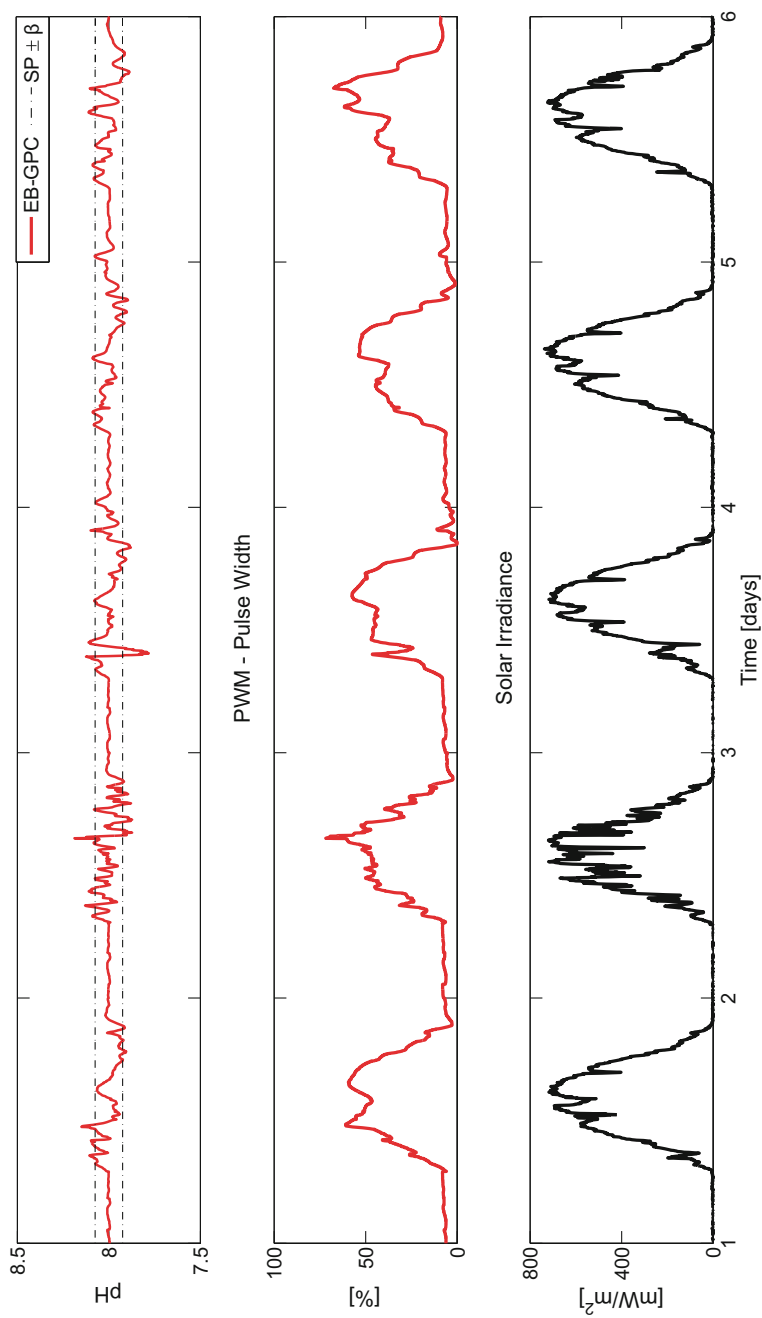


Fig. 10 Experimental event-based control results for a 5-day period (Pawlowski et al. 2014)

a different sampling period (Pawlowski et al. 2012b). Finally, the control weighting factor was adjusted to $\lambda^f = 0.005$ to achieve the desired closed-loop dynamics for the faster GPC controller with $T_1 = T_{base} = 1$ min. Due to the physical limitation of the actuator signal (PWM pulse width), the event-based GPC controller considers constraints on the control signal $0 < u(t) < 100\%$. Taking into account all design parameters, the control structure is composed of five controllers for each possible sampling frequency. Considering pH operating limits for tubular photobioreactor ($7 < \text{pH} < 9$) and the relationship of the pH with the photosynthesis rate (as will be described below), the β parameter was set to $\beta = 0.075$. In such a way, event-based configuration will keep pH close to its optimal value and allows to find an acceptable tradeoff between performance and control effort (Pawlowski et al. 2012b).

It can be observed that for most of the time the controlled variable is inside the established band $SP \pm \beta$. The pH goes outside the band only a few times during the whole test period and this fact is induced by the external disturbances. This is especially visible during the second and third days, where solar irradiance is affected by passing clouds, which changes the photosynthesis rates and affects the pH values. On the other hand, the obtained results show that the event-based controller properly rejects unmeasurable disturbances due to microalgae harvesting action. During clear days, the event-based controller maintains the pH inside the band, updating the process control action at the low rate (with T_{max} sampling time). When the pH crosses the sensor deadband limit, the control structure switches to the fastest sampling frequency T_{base} to move back controlled variable into the set point tolerance band.

Figure 11 shows a detailed view for the fourth day. It can be observed that the event-based GPC provides a good control accuracy. Moreover, it can be seen that each time the pH crosses the sensor deadband, the event-based control system increases the sampling frequency. Additionally, it can be observed how the load disturbance related to harvesting process is rejected properly by event-based controller around the midday. The event-based GPC controller generates less-aggressive control signal as long as the pH is inside the limits. When the controlled variable goes out the limits, the event-based scheme increases sampling frequency to compensate for the disturbances. The bottom graph in Fig. 11 shows how events are generated and can be seen that the event generation frequency increases when the pH goes outside the limit. On the other hand, the sampling frequency decreases when pH is within the limits. In this way, it is possible to reduce the controlled system updates. Hence, as a consequence of the reduced number of process updates, the event-based control system reduces the required control effort related to the CO_2 consumptions as well as CO_2 losses.

Table 1 collects the performance indexes for event-based GPC with sensor deadband in the experimental results. This table shows the Integrated Absolute Error (IAE), the number of events (Event), the Injection Time (IT) in minutes, and the total CO_2 supplied and the CO_2 losses, both expressed in grams. Moreover, two complementary indexes are calculated for oxygen and biomass production, RO_2 and P_b , respectively. Those indexes are used to evaluate analyzed control algorithm and its influence on microalgae culture. The first one is used to express the overall oxygen production rate that is influenced (among others) by solar irradiance and pH.

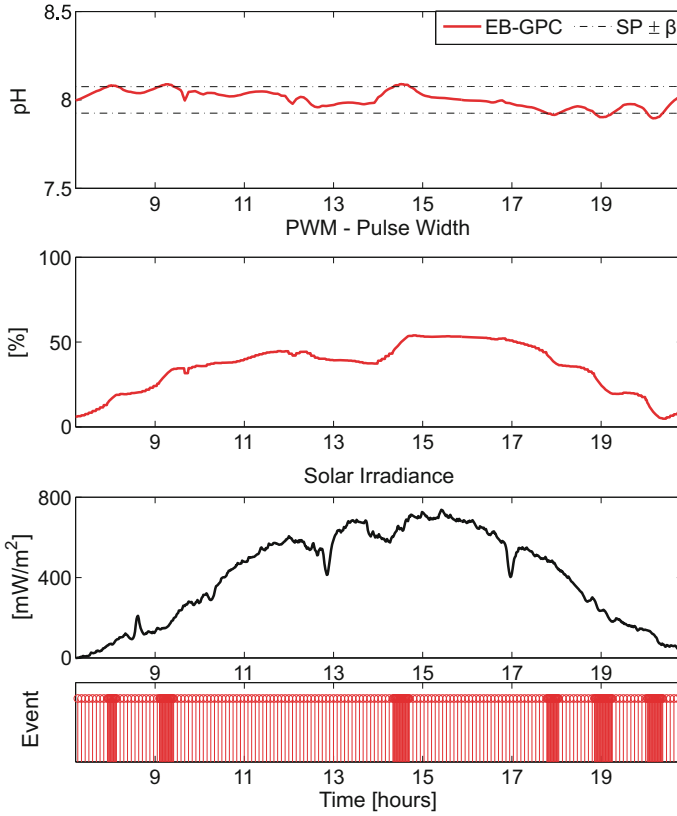


Fig. 11 Experimental control results for event-based GPC for the fourth day (Pawlowski et al. 2014)

Table 1 Event-based control system: performance indexes for the experimental results

		Day				
		1	2	3	4	5
EB-GPC	IAE	1725	1555	1666	1341	1579
	SLT (min)	767	767	767	767	767
	Event	214	280	269	228	258
	IT (min)	319.6	291.1	296.4	284.3	307.8
	CO ₂ (g/day)	1177	1072	1091	1047	1134
	Lost CO ₂ (g/day)	235	216	213	208	227
	RO ₂ (kg _{[O₂]/m³ day)}	0.8464	0.9953	0.9317	0.7526	0.7459
	P _b (kg _[b] /m ³ day)	0.6196	0.7445	0.6783	0.5532	0.5378

The second one shows the biomass production rate (daily measurements), which corresponds to reactor production performance.

It can be observed that the overall IAE index is slightly worst in comparison with those obtained through simulations. This is mainly due to harvesting process that affects the pH control accuracy and was not considered during the simulation study. On the other hand, one can observe how the event-based control scheme reduces the number of events in comparison to the SLT (Solar Light Time), which corresponds to the number of invocation of classical time-based control scheme. The CO_2 usage was similar to the values obtained during simulation study, which confirms the reduction of its usage with respect to the time-based scheme. This fact is also confirmed by the accumulated IT for all considered days. At the same time, it can be seen that the CO_2 losses are reduced. On the other hand, the microalgae growth indexes, RO_2 and P_b , were quite similar for the different days and are comparable with the classical GPC, analyzed previously.

All those benefits are obtained at expense of the control performance taking as a reference of the time-based GPC controller. Moreover, event-based configuration is able to reduce around 30% CO_2 losses obtained by classical GPC. Finally, notice that when event-based GPC controller is compared with on/off controllers (which are the type used in industrial photobioreactor), the control accuracy is highly improved and the CO_2 losses are reduced by more than 2 times.

5.2 Event-Based Controller pH in Raceway Photobioreactor with Efficient CO_2 Usage

The experimenters presented in this section have been performed during 2-week period, between January 27 and February 9, 2014. The analysis is divided into two sets that are related to event-based and on/off control approaches. During the first week, on/off controller was applied for pH control task. The second week was dedicated to event-based GPC evaluation. For both control techniques, the pH reference was set to $w_{pH} = 8$, being optimal for the grown microorganism. The raceway photobioreactor process setup used for this study is shown in Fig. 12. The main objective of these tests is to show the advantages that can be obtained with event-based control technique that focuses on the effective usage of flue gases. It has to be highlighted that the main motivation of this analysis is not a direct comparison of the introduced control techniques, since they are representing two extremely different degrees of complexities as well as different approaches.

5.2.1 On/Off Controller—pH Control Results

In the analyzed period, the pH control task was active only during diurnal periods, since photosynthesis process is active when solar irradiance is available. Moreover,

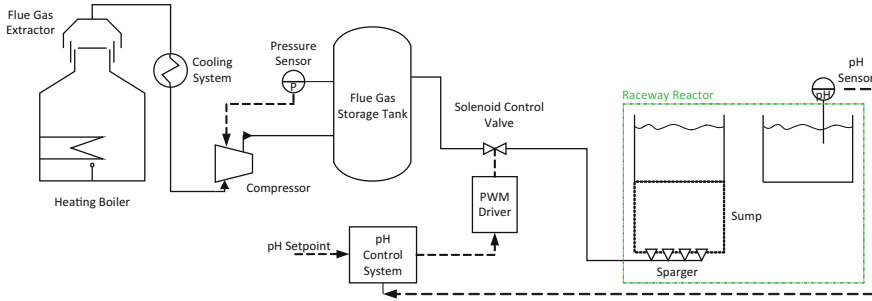


Fig. 12 Raceway reactor with pH control system using flue gases (Pawlowski et al. 2014)

the implementation details are as follows: sampling time was set to 1 min and the control signal is switched between 0 and 100% due to PWM technique. In Fig. 13, the on/off controller results for 7 days period are shown. From this result, it can be observed that on/off regulator maintains the pH level close to the reference. However, the obtained control performance has a low accuracy provoked by the significant pH oscillations (see the first plot in Fig. 13). This issue originates from abrupt changes in control variables (on–off actions). In analyzed configuration, the controller opens the solenoid control valve and applies some flue gases volume until the pH level decreases under selected reference. Once the controlled variable is in the desired range, the on/off controller closes the solenoid value, disabling injection of flue gases. Due to this working principle, a significant oscillation in controlled variable appears, which results in nonoptimal conditions for microalgae culture. The described behavior is present in whole analyzed period (bottom plot in Fig. 13), and appears independently on process disturbances (solar irradiance in this case).

From Fig. 14 (presenting detailed information for the third analyzed day), it can observe the low control performance mainly due to significant oscillations. The presence of these oscillations came from two issues that are not considered by this simple controller. The first one is related to the process dynamics that is not considered in controller structure, and the second is due to plant’s dead time (see Sect. 2.2.1 for details). Those two features of the pH control process result in large control actions that in consequence apply high volume of flue gases, which quickly decreases the pH level. Despite overabundance of CO₂ in cultivation medium, only small part is assimilated by the photosynthesis process. The unabsorbed carbon dioxide is emitted into atmosphere having negative effect on the environment. This issue is of high importance for large-scale industrial photobioreactors, since huge volume of flue gases is needed for the pH control purposes.

Control performance measures for the on/off controller are summarized in Table 2. These measures include the injection time (IT) expressed in minutes, the Integrated Absolute Error (IAE), and the total amount of flue gases (Gas) injected to the raceway photobioreactor. Additionally, the complementary measures related to production rate are computed and contain oxygen production RO_2 , biomass concentration C_b expressed in grams per liter (higher value signify better growth rate), and biomass

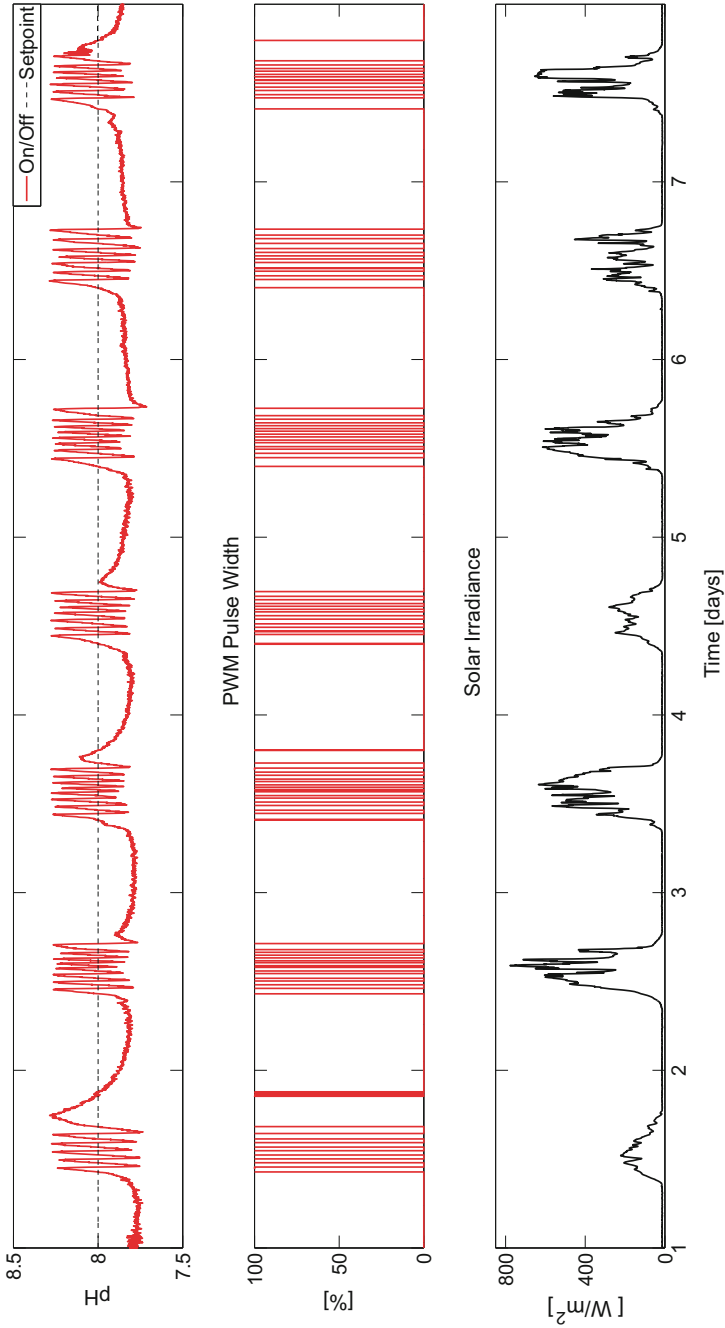


Fig. 13 On/off controller experimental results for a 1-week period (Pawlowski et al. 2014)

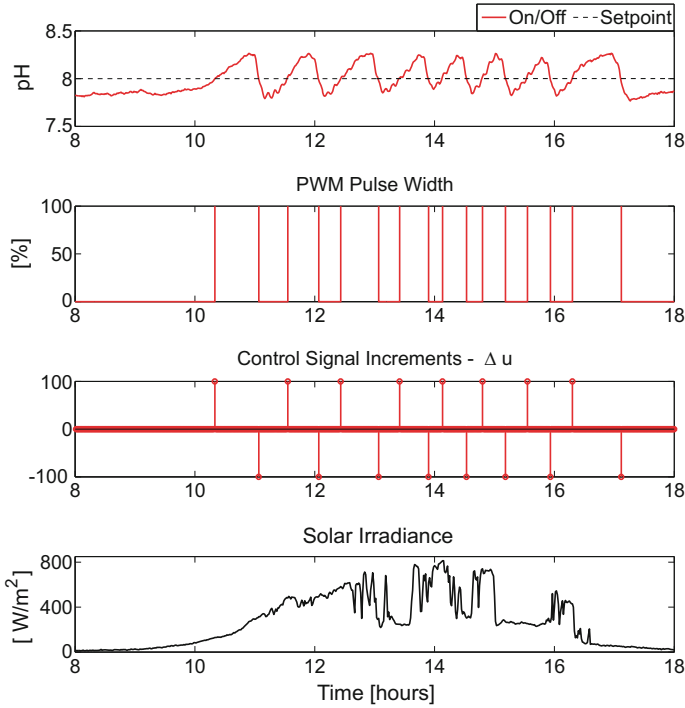


Fig. 14 Experimental results for the third day and on/off controller (Pawlowski et al. 2014)

Table 2 Performance indexes for on/off controller

Day	1	2	3	4	5	6	7
IAE	4503	4232	3436	3749	3945	4158	3678
IT (min)	293	291	298	279	299	290	316
Gas (m ³)	29.3	29.1	29.8	27.9	29.9	29	31.6
RO ₂ (g/m ² day)	7.4	6.8	7	7.2	6.9	7	7.1
C _b (g/l)	0.279	0.240	0.248	0.237	0.238	0.230	0.230
P _b (g/m ² day)	6.2	4.83	5.2	5.7	4.76	4.68	4.68

production P_b (daily measure of the overall performance of the reactor). The RO_2 is computed using dissolved oxygen concentration measure (this index depends on solar irradiance and the pH value) and last two are based on laboratory analysis (Mendoza et al. 2013b). Such indexes are used to show the effect of tested algorithm on microorganism growth performance.

From the obtained values for the IAE index, it can be seen that on/off controller provides low accuracy for whole analyzed period. This is due to significant error between the pH value and the established set point. The IT measure indicates the

average injection time and reaches 280 min per day. The remaining indexes that characterize microalgae growth show an average production rate for this specific year season and on/off controller. Notice that all those measures will be compared with the results obtained using actuator virtual deadband and event-based GPC.

On the other hand, when continuous injection of flue gases is contrasted with on/off controller, the results are more than satisfied. Even this simple control strategy provides on-demand injections reducing volume of supplied flue gases, simultaneously keeping the pH value around the optimal level for culture growth. The atmosphere contamination is considerably lower, since the average volume of supplied flue gases is reduced to about 60%. Based on those indicators, the on/off controller gives a simple solution to decrease the carbon dioxide losses, as well as roughly to regulate the pH value.

Nevertheless, the results obtained with on/off controller can be considerably improved, when advanced control techniques, such as event-based predictive control system, are applied.

5.2.2 Event-Based GPC for pH Control

The event-based scheme was developed by following the methodology shown in Sects. 4.1 and 4.3. The design parameters for corresponding GPC controllers were set up as follows: the control horizon $N_2 = 20$ (capturing main process dynamics), the prediction horizon $N_u = 5$, the weighting factor for control signal $\lambda = 0.05$, and sampling time was set to 60 s. Moreover, to show the influence of actuator virtual deadband on the controlled process, two different values were evaluated. This parameter defines the tradeoff between control accuracy and control effort as well as overall control system performance. Considering these features, the virtual deadbands were established to $\beta_u = 1.5\%$ and $\beta_u = 1\%$ to satisfy control system goals. Additionally, all event-based GPC controllers were implemented with constraints on control signal ($0 < u(t) < 100\%$), due to the limitations defined by the PWM technique.

The introduced event-based GPC was tested during 1-week period on the industrial-scale raceway photobioreactor, and the results are presented in Fig. 15. Analyzing the pH variable, it can be observed that event-based controller improves significantly the control accuracy, when compared to the on/off control strategy. In this case, the pH slowly changes its value and it is kept arrowed the set point with better accuracy. The slow changes are provoked by the solar irradiance that affects the photosynthesis process (increasing the oxygen production), which forces the variations in the pH value. Due to these properties, the solar radiation is treated as control system disturbance and it is handled properly by the event-based controller. Its influence is compensated by controller through control signal increments. On the other hand, the microalgae production process is affected by the harvesting procedure. This action is performed at the midday and can be considered as unmeasurable load disturbance. Despite strong influence on the reactor parameters, the event-based GPC is able to keep the pH level close to established set point.

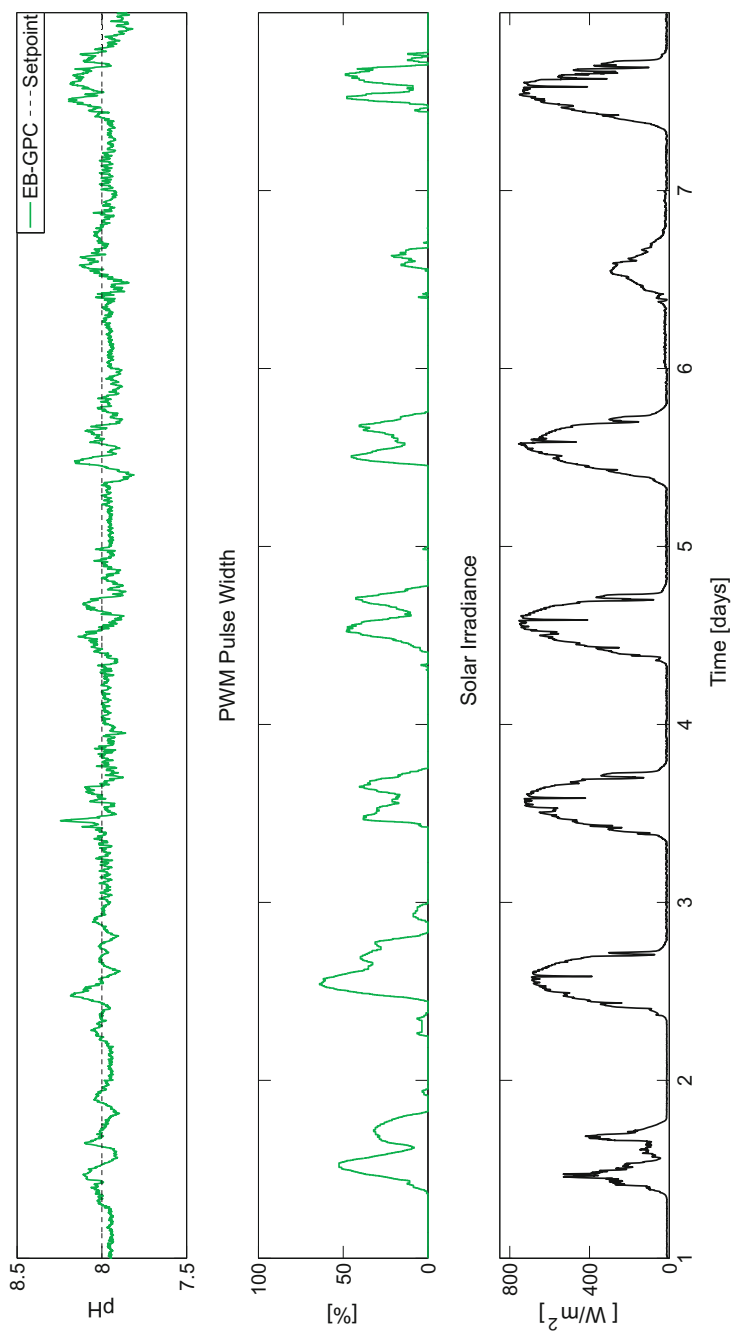


Fig. 15 The EB-GPC controller experimental results for a 1-week period (Pawlowski et al. 2014)

When control results for on/off controller and event-based GPC (shown in Figs. 13 and 15, respectively) are compared, it can be observed that event-based GPC improves control performance (as expected), mainly due to less-aggressive changes in control signal. The control signal provided by the event-based GPC (second plot in Fig. 15) is more smoother and changes gradually counteracting to disturbance dynamics. Moreover, the presence of actuator virtual deadband forces the control signal increments to meet the established minimum and suppressing the small changes, which result in an efficient use of resources. The established deadband is considered in the optimization procedure providing control signal increments bigger than the selected deadband. Due to this feature, it is possible to manage efficiently the volume of flue gases injected to the raceway photobioreactor.

The detailed view for the analyzed event-based controller (for the third day) is shown in Fig. 16. This specific day is characterized by very small variation of the pH (average deviation is less than ± 0.1 from the set point), which creates optimal conditions for microorganism growth. From the control signal (second subplot in Fig. 16), it can be seen how the event-based GPC compensates the photosynthesis effect that influences the pH value. Additionally, the volume of injected flue gases is strictly limited to cover actual demand. Considering this operation mode, it is possi-

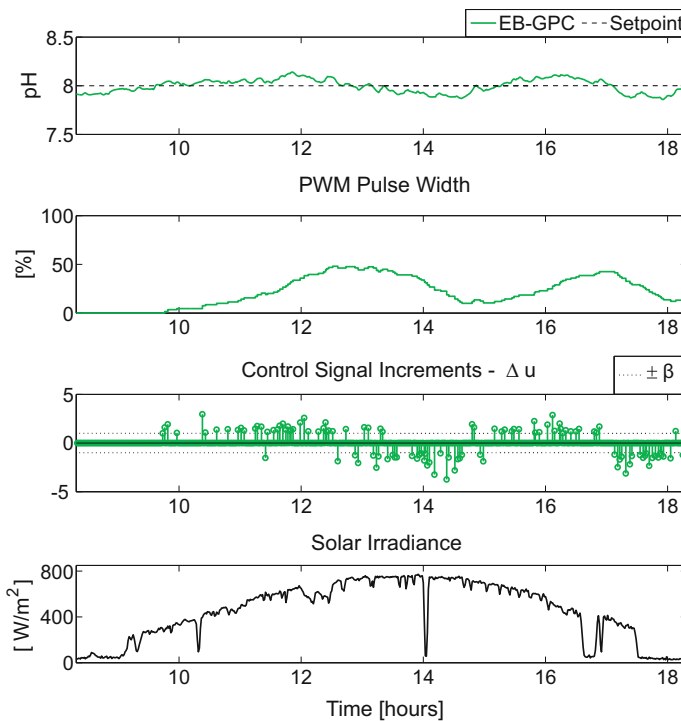


Fig. 16 The EB-GPC controller experimental results for the third day (Pawlowski et al. 2014)

ble to decrease the overall amount of flue gases used for control task, when compared to on/off regulator. The evolution of control signal increments is shown in the third plot, where also deadband value is highlighted. From this plot, it can be observed that all changes in control action are generated outside the established deadband. In consequence, the control system is less sensitive to insignificant error changes that require continuous control signal adjustments. Due to this feature, the event-based controller is able to establish the compromise between control resource utilization and control performance. From the microalgae cultivation process point of view, this property allows efficient use of the flue gases used for control task. In analyzed control scheme, the actuator virtual deadband β_u is used as an additional parameter that needs to be properly adjusted during controller design stage. Such a parameter should be set up taking into account the compromise in resource consumption and control performance. When deadband is set up to small value, the control accuracy is improved at the expense of resource utilization. In the opposite case, setting up the deadband to high value, it is possible to decrease the control resource utilization, which results in lower control accuracy.

Table 3 summarizes the control performance measures for event-based GPC evaluation. As mentioned previously, two different deadband values were used to test its influence. During first 2 days, $\beta_u = 1$ were used, and afterward its value was changed to 1.5. The computed IAE values for first 2 days are lower when compared to the days with $\beta_u = 1.5$ (verifying previously features for event-based controller). Independent on the deadband value, the IAE index is significantly improved in comparison to the on/off regulator, gaining about 50% in control system accuracy. Moreover, the average value of IT index was reduced over 40%, and simultaneously the amount of the used flue gases is also minimized. Taking into account these features, the event-based control scheme allows to improve control performance and reduce the volume of the flue gases used for control purposes. The last feature is of high importance for large-scale photobioreactors, since the volume of carbon dioxide wastage is minimized. As a consequence, event-based controller prevents the emission of important volume of greenhouse gases into atmosphere. It should be highlighted that the event-based control approach improves the CO₂ fixation through the efficient management of flue gases.

Table 3 Performance indexes for event-based GPC controller

Day	1	2	3	4	5	6	7
β_u [%]	1	1	1.5	1.5	1.5	1.5	1.5
IAE	1525	1661	1817	2239	2098	1569	2241
IT (min)	222	269	189	183	159	82	165
Gas (m ³)	22.2	26.9	18.9	18.3	15.9	8.2	16.5
RO ₂ (g/m ² day)	10.6	11.7	12.5	10.6	13.3	11.5	14.8
C _b (g/l)	0.329	0.321	0.341	0.349	0.384	0.367	0.395
P _b (g/m ² day)	7.85	7.19	8.14	6.50	8.22	7.36	8.85

On the other hand, the improved control system performance has a beneficial influence on the microorganism growth rate. All related measures (RO_2 , C_b , and P_b) were improved. The average RO_2 value increased about 50% in comparison to its average value for on/off control technique. In the case of biomass concentration, this index was improved around 30%. The P_b measure also gets better obtaining average value of $7.6 \text{ g/m}^2 \text{ day}$. Considering all these results, it is demonstrated that evaluated event-based controller allows to improve the pH control accuracy in race reactor (keeping the optimal cultivation conditions) and also provides the effective usage of flue gases.

5.3 Selective Event-Based Controller for pH and Dissolved Oxygen in Raceway Photobioreactor

In this section, the evaluation of the selective event-based control system is presented. Resulting raceway photobioreactor setup for such a scheme is shown in Fig. 17, where the pH process is controlled with flue gases and dissolved oxygen is regulated using compressed air.

The experimental evaluation was performed for 1-week period (from July 20 to July 27, 2014). Selected time period allows us to test the implemented selective event-based scheme during diverse solar irradiance profiles, providing reliable results. The control scheme was developed using the approach presented in Sect. 4.4. In this scheme, the pH process is controlled by event-based GPC and dissolved oxygen is regulated by on/off control technique. The event-based GPC relies on process model and the first step in control system development was devoted to capture the dynamics between the pH value and carbon dioxide injections. Once the process model was determined (see Sect. 4.4), the control structure was ported to raceway reactor SCADA system.

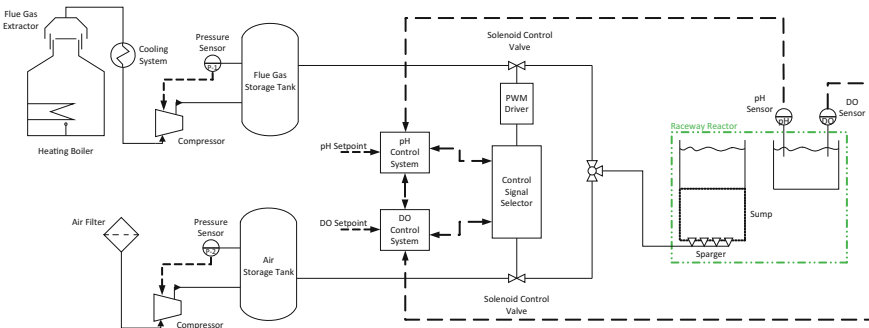


Fig. 17 Selective control scheme: raceway reactor setup for the pH and dissolved oxygen control (Pawlowski and Mendoza 2015)

The GPC structure was implemented with the following setup: the prediction horizon was set to $N_2 = 20$, the control horizon N_u was set to 5, and the control signal weighting factor $\lambda = 0.05$. The sampling time was established to 1 min, considering process dynamics. Moreover, following the results from (Pawlowski et al. 2014), the actuator virtual deadband β_u was set to 1.5. Due to the PWM technique, the GPC optimization procedure includes the constraints on control signal ($u_{pH} \in 0-100\%$). As shown in the previous section, the actuator deadband provides the possibility to establish the tradeoff between control system accuracy and control system effort (flue gas usage in this case). For this study, the pH reference was set to 7.7 and for the dissolved oxygen, set point was selected to 150 [%Sat]. The dissolved oxygen was controlled with on/off technique (with 1 min sampling time) provided on-demand injection of compressed air.

Regarding the selective control parameters, the switching condition (see Eq. 12) was implemented using $SCSP_{pH} = 8$, with tolerance $\pm\beta = 0.3$ and reference for dissolved oxygen was set up to $SCSP_{DO} = 200$ [%Sat]. Following the selective control working principle, the pH value will be kept within set point ± 0.3 interval and this tolerance will enable the possibility to maintain the dissolved oxygen concentration under the dangerous value. In such a case, the dissolved oxygen control task has a lower priority and is executed only when the pH level is inside the selected limits. As shown previously, the provided tolerance has an insignificant influence on photosynthesis rate and, in this approach, is exploited to provide dissolved oxygen control. Being an important advantage, the oxygen concentration is kept under the limit, which in consequence improves the photosynthesis rate and volume of biomass production.

The results obtained from the analyzed system are shown in Fig. 18. From the first plot, it can be observed that pH level is controlled within the established limit and only during nocturnal periods drop under the band (photosynthesis process is not active during the night and no pH control is performed). Additionally, it can be seen how the event-based GPC handles the changes in solar irradiance (main control system disturbance), which is reflected in the control signal that captures variations in solar irradiance (Fig. 18). Moreover, from the pH control signal, it can be observed how the switching mechanism operates. In certain situations, the pH control signal is switched to zero and then controller for dissolved oxygen is activated. This is due to raceway reactor shared by actuation structure, which can change the injected gas type (atmospheric air or flue gases). The swapping action between two controllers is activated when the event-based triggering condition meets the logical sequence (Eq. 12 in Sect. 4.4). Due to this working principle, two controllers can be executed in parallel, meeting diverse control system objects that can be with classic approach. This operation mode is confirmed by the changes in control for pH and dissolved oxygen (second and fourth plots, respectively).

The control results for dissolved oxygen control subsystem are shown in third and fourth plots in Fig. 18. For this specific variable, the on/off controller provides compressed air injections to reduce the oxygen concentration. The obtained results show the efficacy of devolved control scheme, since the dissolved oxygen is kept below the established limit (200 [%Sat]). It should be highlighted that dissolved oxygen

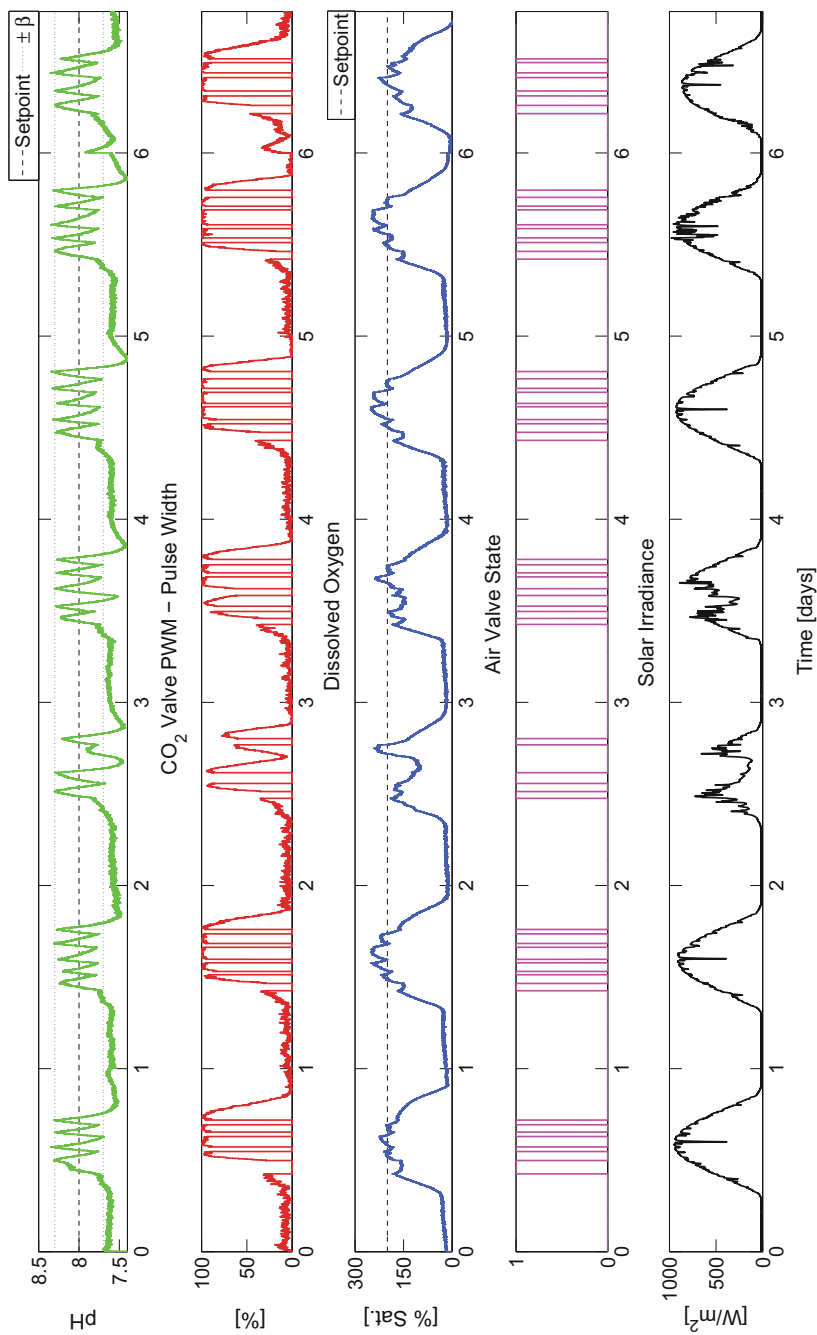


Fig. 18 Experimental results of the selective control strategy with the event-based approach for pH and dissolved oxygen control (Pawlowski and Mendoza 2015)

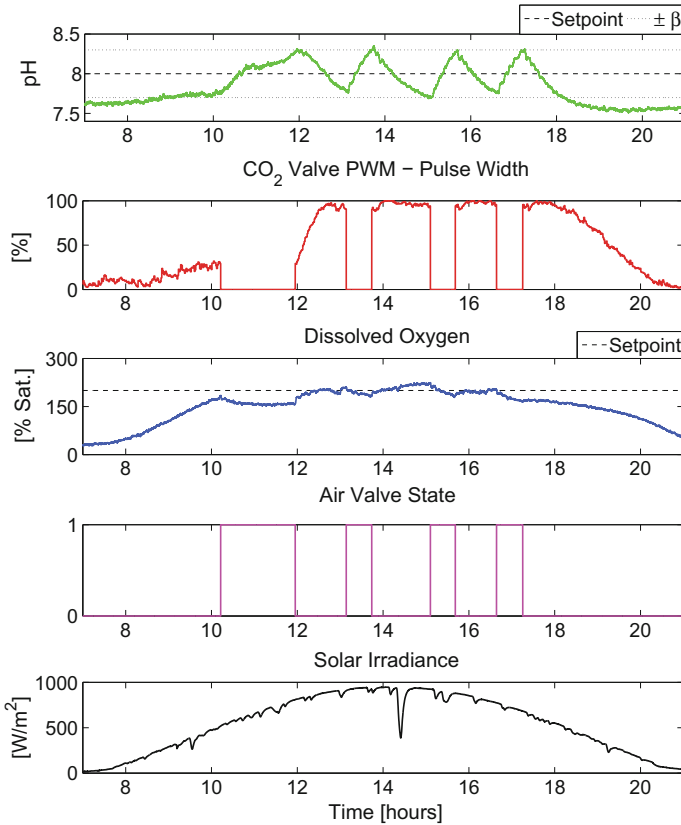


Fig. 19 Selective control details for the first day—solar irradiance without clouds (Pawlowski and Mendoza 2015)

concentration rarely exceeds the 250 [%Sat], which is marked as the dangerous limit. This situation is beneficial for the microalgae growth, since the cultivation process is performed in optimal conditions.

The day presented in Fig. 19 is characterized by stable solar irradiance, which stimulates the photosynthesis process. From the first plot, it can be observed that the pH value is maintained inside the tolerance band despite high solar irradiance. Due to high photosynthesis rate, the event-based GPC provides a high amount of flue gases to deliver necessary carbon dioxide and to reduce the pH level. During this specific day, the control system operates close to the upper saturation limit. From the dissolved oxygen point of view, its value is kept below the critical value for most of the day. Nevertheless, during central hours of the day, its value exceeds for few minutes above this established limit. This is due to the photosynthesis process peaked that results in high dissolved oxygen concentration. The main reason of this excess is due to the pH prioritization, since this parameter is critical in cultivation process.

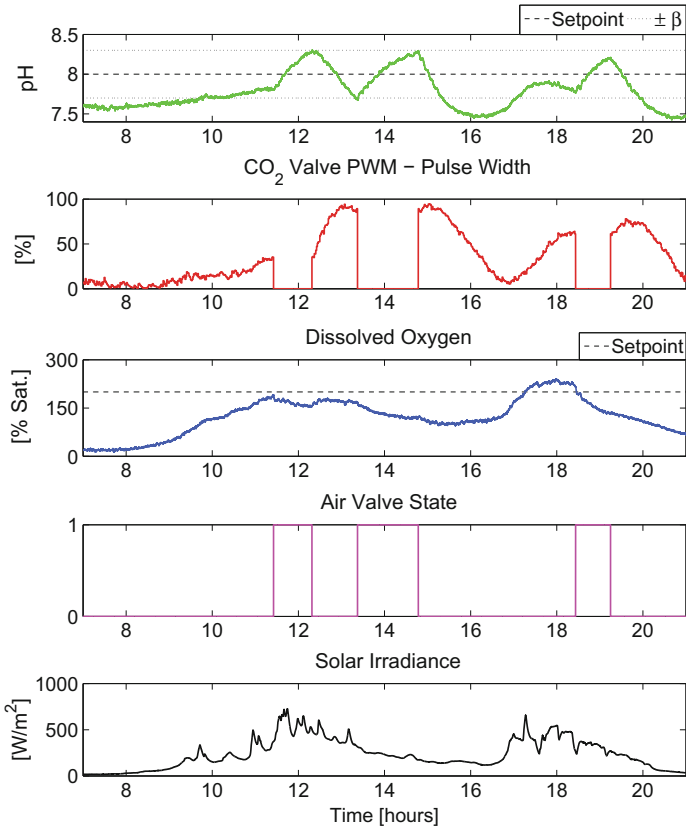


Fig. 20 Selective control details for the third day—solar irradiance with passing clouds (Pawlowski and Mendoza 2015)

Despite this insignificant issue, both variables are close to the optimal values, thanks to the selective event-based control approach.

The second analyzed day (see Fig. 20) is characterized by strong variations in solar irradiance, due to passing clouds, and is used to show how the event-based selective control reacts to disturbances. From such figure, it can be seen that until 12 am control system provides good control accuracy for both variables. This situation changes between 14 and 16 h, since the system perturbation (solar irradiance) abruptly changes the value affecting the microorganism production rate. In consequence, the pH value moves outside the selected band. However, the event-based GPC reacts decreasing the volume of injected flue gases in order to increase the pH. During this action, the selective controller focuses on the pH value (being more important) and once recovered its optimal value also handles the dissolved oxygen. Moreover, from the control signal for the dissolved oxygen, it can be observed that compressed air is provided to the raceway photobioreactor only when necessary.

Table 4 Performance indexes for the selective control strategy with the event-based approach

Day	1	2	3	4	5	6	7
IAE_{pH}	108	84	118	97	80	83	95
IT (min)	298	352	194	314	342	340	342
Gas (m^3)	29.8	35.2	19.4	31.4	34.2	34.0	34.2
IAE_{DO}	1441	1601	2969	1791	1620	1693	2270
DO_{OLT} (min)	111	264	64	65	259	254	56
RO_2 (g/m^2 day)	25.7	25.8	32.4	30.7	29.9	28.8	28.3
C_b (g/l)	0.57	0.74	0.64	0.63	0.62	0.63	0.63
P_b (g/m^2 day)	17.5	20.6	23.5	17.4	20.2	19.4	18.7

This feature is important from the economic point of view, since it allows us reducing maintenance costs when compared to the system with continuous aeration system.

The control performance indexes for analyzed scheme are summarized in Table 4. These measures include IAE_{DO} and IAE_{pH} —integrated absolute errors (for pH and dissolved oxygen, respectively), IT —the injection time in minutes, Gas —volume of flue gases injected to the photobioreactor, and DO_{OLT} —the amount of time when dissolved oxygen measure is over the limit (200 [%Sat]). Additionally, three measures related to the microalgae production were computed: RO_2 —oxygen production, P_b —biomass production, and C_b —biomass concentration expressed in grams per liter, respectively. The RO_2 index is computed using the dissolved oxygen measures and it is proportional to photosynthesis rate (Mendoza et al. 2013b). The last two were obtained from laboratory study. All these indexes are used to the influence of event-based selective control on the microorganism growth.

Analyzing the IAE measures, it can be observed that control accuracy is significantly higher for pH variable. This is due to selective control configuration, where the pH is prioritized over the dissolved oxygen. Additionally, the event-based GPC scheme is able to use the control resources (flue gases in this case), minimizing the overall supplied volume (see IT measure). Nevertheless, this control performance is lower when compared to the classical control approach that handles the pH individually. On the other hand, the selective control system is able to control both parameters at the expense of control accuracy deterioration. This operation mode allows us to establish the tradeoff between the pH and dissolved oxygen control accuracy and can be exploited to simultaneous control of both variables. Due to these properties, it is demonstrated that simple on/off regulator can maintain oxygen concentration under the danger limit. The DO_{OLT} index shows that the dissolved oxygen is inside the safe zone and rarely exceed the 250 [%Sat]. Another important feature of event-based selective control is related to energy savings in aeration system, since the compressed air is applied when strictly necessary. The results provided for industrial-scale reactor are satisfactory, since both variables are kept around their optimal values. Moreover, the analyzed control system is able to address several issues related to maintenance costs and efficient use of control resources, using standard reactor architecture.

Taking into account these features, the event-based selective control scheme provides a unified solution for simultaneous control of the pH and dissolved oxygen.

The microorganism cultivation indexes indicate very good growth conditions due to the application of event-based selective control approach. It needs to be mentioned that the average biomass production rate (P_b) and biomass concentration show C_b for common control approach (on/off regulator for pH variable) are around 17 and 0.57, respectively, whereas the analyzed control technique improved the overall photobioreactor productivity around 15% (average value for all indexes) for 1-week period. Notice that these results can be extrapolated for large-scale photobioreactors and result in increased productivity of raceway reactor.

6 Summary

In this chapter, the practical evaluation of event-based control schemes for industrial photobioreactors was analyzed. This study considers three different configurations that were implemented for control tasks in microalgae culture process.

In the first analyzed configuration, an event-based GPC control strategy has been used to reduce CO₂ losses in pH control of tubular photobioreactors by keeping an adequate control performance level. The core idea consists of updating the controlled process only when significant deviations from the set point occur. The presented control scheme provides savings in plant maintenance cost, minimizing the CO₂ losses. The obtained benefits are reached at the expense of control performance through control accuracy degradation. The desired tradeoff between control performance and CO₂ losses can be easily implemented adjusting a sensor deadband value at the control system design stage. The experiments show that the event-based GPC control scheme is suitable for pH control in tubular photobioreactors. The obtained reductions in CO₂ losses are even more significant than in the case of classical GPC analyzed in Berenguel et al. (2004). This is due to the event-based framework, which allows to reduce the resource utilization at expense of the control performance. In such case, it is possible to meet the compromise between control accuracy degradation and plant maintenance costs as well as environmental impact. The evaluation performed in this study is based on a single photobioreactor, but it can be easily extrapolated to industrial scale. In such case, the benefits are even more visible.

The second analyzed event-based control scheme provides interesting results on the efficient use of the flue gases in microalgae cultivation process. The event-based GPC with actuator virtual deadband allows to decrease the volume of injected flue gases into raceway photobioreactor when collated with results for commonly used controller. Performed evaluation demonstrated that the use of event-based approach in raceway reactor process improves the growth rate, since the cultivation conditions are improved through better control accuracy. Additionally, tested configurations supply significantly smaller flue gases volume due to its efficient management in controller task.

The last studied event-based approach addresses the pH and dissolved oxygen control problems simultaneously using a unified structure. To this end, the event-based selective control scheme is applied to raceway photobioreactor. The results of the experimental evaluation show that implemented control algorithm is able to handle both variables providing good control performance. Due to event-based system properties, the analyzed control scheme is able to adapt dynamically to the photosynthesis rate. Additionally, this property provides the mechanism to detect changes in the process state and is used as a trigger to switch between dissolved oxygen and pH controllers. In tested approach, the event-based GPC uses efficiently the flue gases (CO_2 source) for pH control and an on/off regulator reduces energy usage providing demand compressed air injections (for dissolved oxygen control). The application of event-based control scheme increases the microalgae production performance, since the growth parameters were kept close to its optimal values and the selective scheme allows us the optimization of the raceway production process.

From the obtained results, it can be seen that all evaluated event-based configurations improve the control accuracy (when compared to the commonly used controllers), while preserving the control resources. Taking into account all features and properties of tested event-based approaches, a great potential to improve the production rate is observed. However, the future effort for long-term evaluation as well as theoretical studies is required to make the event-based control approach widely accepted in the bioprocess industry.

Acknowledgements This work has been partially funded by the following projects: DPI2014-55932-C2-1-R, DPI2014-55932-C2-2-R, DPI2014-56364-C2-1-R, and DPI2012-31303 (financed by the Spanish Ministry of Economy and Competitiveness and EU-ERDF funds); Controlcrop P10-TEP-6174 (financed by the Consejería de Economía, Innovación y Ciencia de la Junta de Andalucía); and the UNED through a postdoctoral scholarship.

References

- Ación FG, Fernández JM, Magán JJ, Molina E (2012) Production cost of a real microalgae production plant and strategies to reduce it. *Biotechnol Adv* 30:1344–1353
- Ación FG, Fernández JM, Sánchez JA, Molina E, Chisti Y (2001) Airlift-driven external-loop tubular photobioreactors for outdoor production of microalgae: assessment of design and performance. *Chem Eng Sci* 56(8):2721–2732
- Ación FG, García F, Chisti Y (1999) Photobioreactors: light regime, mass transfer, and scale-up. *Prog Ind Microbiol* 35:231–247
- Ación FG, González-López CV, Fernández JM, Molina E (2012) Conversion of CO_2 into biomass by microalgae: how realistic a contribution may it be to significant CO_2 removal? *Appl Microbiol Biotechnol* 96:577–586
- Årzén KE (1999) A simple event-based PID controller. In: *Proceedings of the 14th IFAC World Congress, Beijing, China*
- Åström KJ (2007) Event based control. In: *Analysis and design of nonlinear control systems*, Springer
- Bemporad A, Morari M (1999) Control of systems integrating logic, dynamics, and constraints. *Automatica* 35:407–427

- Beneman J, Tillet D, Weissman J (1987) Microalgal biotechnology. *Trends Biotechnol* 5:47–53
- Berenguel M, Rodríguez F, Ación FG, García JL (2004) Model predictive control of pH in tubular photobioreactors. *J Process Control* 14:377–387
- Bernard O (2011) Hurdles and challenges for modelling an control of microalgae for CO₂ mitigation and biofuel prediction. *J Process Control* 21:1378–1389
- Beschi M, Dormido S, Sánchez J, Visioli A (2012) Characterization of symmetric send-on-delta PI controllers. *J Process Control* 22(10):1930–1945
- Beschi M, Pawlowski A, Guzmán JL, Berenguel M, Visioli A (2014) Symmetric send-on-delta PI control of a greenhouse system. In: *Proceedings of the 19th IFAC World Congress, Cape Town, South Africa*
- Brennan L, Owende P (2010) Biofuels from microalgae—a review of technologies for production, processing, and extractions of biofuels and co-products. *J Biosci Bioeng* 14:217–232
- Cai T, Wang S, Xu Q (2013) Scheduling of multiple chemical plant start-ups to minimize regional air quality impacts. *Comput Chem Eng* 54:68–78
- Camacho EF, Bordóns C (2007) *Model predictive control*. Springer, London
- Camacho F, Ación FG, Sánchez JA, García F, Molina E (1999) Prediction of dissolved oxygen and carbon dioxide concentration profiles in tubular photobioreactors for microalgal culture. *Biotechnol Bioeng* 62(1):71–86
- Charpentier JC (2009) Perspective on multiscale methodology for product design and engineering. *Comput Chem Eng* 33:936–946
- Chiaramonti D, Prussi M, Casini D, Tredici MR, Rodolfi L, Bassi N, Zittelli GC, Bondioli P (2013) Review of energy balance in raceway ponds for microalgae cultivation: re-thinking a traditional system is possible. *Appl Energy* 102(4):101–111
- Chisti Y (2007) Biodiesel from microalgae. *Biotechnol Adv* 1(25):294–306
- Christofides PD, Scattolini R, Muñoz de la Peña D, Liue J (2013) Distributed model predictive control: a tutorial review and future research directions. *Comput Chem Eng* 51:21–41
- Costache TA, Ación FG, Morales MM, Fernández-Sevilla JM, Stamatini I, Molina E (2013) Comprehensive model of microalgae photosynthesis rate as a function of culture conditions in photobioreactors. *Appl Microbiol Biotechnol* 97(17):7627–7637
- Doucha J, Straka F, Lívanský K (2005) Utilization of flue gas for cultivation of microalgae (*Chlorella* sp.) in an outdoor open thin-layer photobioreactor. *J Appl Phycol* 17:403–412
- Fernández I, Peña J, Guzmán JL, Berenguel M, Ación FG (2010) Modelling and control issues of pH in tubular photobioreactors. In: *Proceedings of the 11th IFAC symposium on computer applications in biotechnology, Leuven, Belgium*
- Ferre JA, Pawlowski A, Guzmán JL, Rodríguez F, Berenguel M (2010) A wireless sensor network for greenhouse climate monitoring. In: *Proceedings of the fifth international conference on broadband and biomedical communications, Malaga, Spain*
- Freudenberg J, Middleton R (1999) Properties of single input, two output feedback systems. *Int J Control* 72(16):1446–1465
- García JL, Berenguel M, Rodríguez F, Fernández JM, Brindley C, Ación FG (2003) Minimization of carbon losses in pilot-scale outdoor photobioreactors by model-based predictive control. *Biotechnol Bioeng* 84:533–543
- de Godos I, Mendoza JL, Ación FG, Molina E, Banks CJ, Heaven S, Rogalla F (2014) Evaluation of carbon dioxide mass transfer in raceway reactors for microalgae culture using flue gases. *Biores Technol* 153:307–314
- Han HG, Qiao JF, Chen QL (2012) Model predictive control of dissolved oxygen concentration based on a self-organizing RBF neural network. *Control Eng Pract* 20:465–476
- Hu Q, Kurano N, Kawachi M, Iwasaki I, Miyachi S (1998) Ultrahighcell-density culture of a marine green alga *Chlorococcum littorale* in a flat-plate photobioreactor. *Appl Microbiol Biotechnol* 49:655–662
- Hu Y, El-Farra NH (2011) Resource-aware model predictive control using adaptive sampling. In: *Proceedings of the annual meeting of American institute of chemical engineers, Minneapolis, USA*

- Johnsson O, Sahlin D, Linde J, Lidén G, Hägglund T (2015) A mid-ranging control strategy for non-stationary processes and its application to dissolved oxygen control in a bioprocess. *Control Eng Pract* 42:89–94
- Kokossis AC, Yang A (2010) On the use of systems technologies and a systematic approach for the synthesis and the design of future biorefineries. *Comput Chem Eng* 34:1397–1405
- Laws EA, Berning JL (1991) A study of the energetics and economics of microalgal mass culture with the marine chlorophyte *tetraselmis suecica*: implications for use of power plant stack gases. *Biotechnol Bioeng* 37(4):936–947
- Lazar C, Pintea R, Keyser RD (2007) Nonlinear predictive control of a pH process. In: Proceedings of 17th European symposium on computer aided process engineering ESCAPE17, Bucharest, Romania
- Liptak BG (2004) Instrument engineers' handbook, 4th edn. Volume two: process control and optimization. CRC Press, London
- Marquez FJ, Sasaki K, Nishio N, Nagai S (1995) Inhibitory effect of oxygen accumulation on the growth of *spirulina platensis*. *Biotechnol Lett* 17:225–228
- Mendoza JL, Granados MR, de Godos I, Ación FG, Molina E, Banks CJ, Heaven S (2013a) Fluid-dynamic characterization of real-scale raceway reactors for microalgae production. *Biomass Bioener* 54:267–275
- Mendoza JL, Granados MR, de Godos I, Ación FG, Molina E, Heaven S, Banks CJ (2013b) Oxygen transfer and evolution in microalgal culture in open raceways. *Bioresour Technol* 137:188–195
- Miskowicz M (2006) Send-on-delta concept: an event-based data reporting strategy. *Sensors* 1:29–63
- Oblak S, Skrjanc I (2010) Continuous-time Wiener-model predictive control of a pH process based on a PWL approximation. *Chem Eng Sci* 65:1720–1728
- Oswald WJ, Golueke CG (1960) Biological transformation of solar energy. *Adv Appl Microbiol* 2:223–262
- Pawlowski A, Cervin A, Guzmán JL, Berenguel M (2014) Generalized predictive control with actuator deadband for event-based approaches. *IEEE Trans Ind Inform* 10(1):523–537
- Pawlowski A, Fernández I, Guzmán JL, Berenguel M, Ación FG, Normey-Rico JE (2014) Event-based predictive control of pH in tubular photobioreactors. *Comput Chem Eng* 65:28–39
- Pawlowski A, Fernández I, Guzmán JL, Berenguel M, Ación FG, Dormido S (2016) Event-based selective control strategy for raceway reactor: a simulation study. In: Proceedings of the 11th IFAC symposium on dynamics and control of process systems, including Biosystems—DYCOPS-CAB 2016, Trondheim, Norway
- Pawlowski A, Guzmán JL, Berenguel M, Dormido S (2014b) Lagrange interpolation for signal reconstruction in event-based gpc. In: Proceedings of the 19th IEEE international conference on emerging technologies and factory automation, Barcelona, Spain
- Pawlowski A, Guzmán JL, Berenguel M, Dormido S (2015) Event-based generalized predictive control. In: Event-based control and signal processing pp 151–176
- Pawlowski A, Guzmán JL, Normey-Rico JE, Berenguel M (2012a) Improving feedforward disturbance compensation capabilities in generalized predictive control. *J Process Control* 22(3):527–539
- Pawlowski A, Guzmán JL, Normey-Rico JE, Berenguel M (2012b) A practical approach for generalized predictive control within an event-based framework. *Comput Chem Eng* 41:52–66
- Pawlowski A, Guzmán JL, Rodríguez F, Berenguel M, Sánchez J, Dormido S (2009) The influence of event-based sampling techniques on data transmission and control performance. In: Proceedings of the 14th IEEE international conference on emerging technologies and factory automation, Mallorca, Spain
- Pawlowski A, Mendoza JL, Guzmán JL, Berenguel M, Ación FG, Dormido S (2015) Selective pH and dissolved oxygen control strategy for a raceway reactor within an event-based approach. *Control Eng Pract* 44:209–218

- Pawlowski A, Mendoza JL, Guzmán JL, Berenguel M, Acién FG, Dormido S (2014) Effective utilization of flue gases in raceway reactor with event-based pH control for microalgae culture. *Bioresour Technol* 170:1–9
- Pawlowski A, Rodríguez C, Guzmán JL, Berenguel M, Dormido S (2016) Measurable disturbances compensation: analysis and tuning of feedforward techniques for dead-time processes. *Processes* 4(2):12
- Peng L, Lan CQ, Zhang Z (2013) Evolution, detrimental effects, and removal of oxygen in microalga cultures: a review. *AIChE Environ Prog Sustain Energy* 32(4):982–988
- Posten C (2009) Design principles of photo-bioreactors for cultivation of microalgae. *Eng Life Sci* 9:165–177
- Putt R, Singh M, Chinnasamy S, Das KC (2011) An efficient system for carbonation of high-rate algae pond water to enhance CO₂ mass transfer. *Bioresour Technol* 102:3240–3245
- Richmond A (2004) Principles for attaining maximal microalgal productivity in photobioreactors: an overview. *Hydrobiologia* 512(1–3):33–37
- Romero-García JM, Guzmán JL, Moreno JC, Acién FG, Fernández-Sevilla JM (2012) Filtered Smith Predictor to control pH during enzymatic hydrolysis of microalgae to produce l-aminoacids concentrates. *Chem Eng Sci* 82:121–131
- Sánchez J, Visioli A, Dormido S (2011) A two-degree-of-freedom PI controller based on events. *J Process Control* 21:639–651
- Santabarbara S, Cazzalini I, Rivadossi A, Garlaschi FM, Zucchelli G, Jennings RC (2002) Photoinhibition in vivo and in vitro involves weakly coupled chlorophyllprotein complexes. *Photochem Photobio* 75:613–618
- Senthil KA, Zainal A (2012) Model predictive control (MPC) and its current issues in chemical engineering. *Chem Eng Commun* 199:472–511
- Sierra E, Acién FG, Fernández J, García J, González C, Molina E (2008) Characterization of a flat plate photobioreactor for the production of microalgae. *Chem Eng J* 138:136–147
- Smith CA (2002) Automated continuous process control. Wiley
- Sompech K, Chisti Y, Srinophakun T (2012) Design of raceway ponds for producing microalgae. *Appl Energy* 3(4):387–397
- Soria-López A, Martínez-García JC, Aguilar-Ibañez CF (2013) Experimental evaluation of regulated non-linear under-actuated mechanical systems via saturation-functions-based bounded control: the cart pendulum system case. *IET Control Theory Appl* 7(12):1642–1650
- Spolaore P, Joannis-Cassan C, Duran E, Isambert A (2006) Commercial applications of microalgae. *J Biosci Bioeng* 101:87–96
- Su Z, Kang R, Shi S, Cong W, Cai Z (2008) An economical device for carbon supplement in large-scale micro-algae production. *Bioprocess Biosyst Eng* 31(6):641–645
- Tang D, Han W, Li P, Miao X, Zhong J (2011) CO₂ biofixation and fatty acid composition of *Scenedesmus obliquus* and *Chlorella pyrenoidosa* in response to different CO₂ levels. *Bioresour Technol* 102:3071–3076
- Taras S, Woinaroschy A (2012) An interactive multi-objective optimization framework for sustainable design of bioprocesses. *Comput Chem Eng* 43:10–22
- Ugwu CU, Aoyagi H, Uchiyama H (2007) Influence of irradiance, dissolved oxygen concentration, and temperature on the growth of *Chlorella sorokiniana*. *Photosynthetica* 45:309–311
- Wang B, Lan CQ, Horsman M (2012) Closed photobioreactors for production of microalgal biomasses. *Biotechnol Adv* 30:904–912
- Weissman JC, Goebel RP (1987) Design and analysis of pond system for the purpose of producing fuels. Final Report, 231-2840 edn. Solar Energy Research Institute, Golden CO, SERI/STR
- Weissman JC, Goebel RP, Benemann JR (1988) Photobioreactor design: mixing, carbon utilization, and oxygen accumulation. *Biotechnol Bioeng* 31(4):336–344
- Zhang K, Miyachi S, Kurano N (2001) Photosynthetic performance of a cyanobacterium in a vertical flat-plate photobioreactor for outdoor microalgal production and fixation of CO₂. *Biotechnol Lett* 23:21–26